EPA/635/R-10/002C
www.epa.gov/iris

TOXICOLOGICAL REVIEW OF FORMALDEHYDE INHALATION TOXICITY

(CAS No. 50-00-0)

In Support of Summary Information on the Integrated Risk Information System (IRIS)

VOLUME I of IV

Introduction, Background, and Toxicokinetics

March 17, 2010

NOTICE

This document is an ***Inter-Agency Science Consultation review draft***. This information is distributed solely for the purpose of pre-dissemination peer review under applicable information quality guidelines. It has not been formally disseminated by EPA. It does not represent and should not be construed to represent any Agency determination or policy. It is being circulated for review of its technical accuracy and science policy implications.

U.S. Environmental Protection Agency
Washington, DC

DISCLAIMER

This document is a preliminary draft for review purposes only. This information is distributed solely for the purpose of pre-dissemination peer review under applicable information quality guidelines. It has not been formally disseminated by EPA. It does not represent and should not be construed to represent any Agency determination or policy. Mention of trade names or commercial products does not constitute endorsement or recommendation for use.

CONTENTS—TOXICOLOGICAL REVIEW OF FORMALDEHYDE
(CAS No. 50-00-0)

VOLUME I

CONTENTS (continued)

VOLUME II

CONTENTS (continued)

CONTENTS (continued)

CONTENTS (continued)

VOLUME III

CONTENTS (continued)

CONTENTS (continued)

VOLUME IV

CONTENTS (continued)

LIST OF TABLES

LIST OF TABLES (continued)

LIST OF TABLES (continued)

LIST OF TABLES (continued)

LIST OF TABLES (continued)

LIST OF TABLES (continued)

LIST OF TABLES (continued)

LIST OF TABLES (continued)

LIST OF TABLES (continued)

LIST OF FIGURES

LIST OF FIGURES (continued)

LIST OF FIGURES (continued)

LIST OF FIGURES (continued)

LIST OF FIGURES (continued)

LIST OF ABBREVIATIONS AND ACRONYMS

ACGIH	American Conference of Governmental Industrial Hygienists
ADAF	age-dependent adjustment factors
ADH	alcohol dehydrogenase
ADS	anterior dorsal septum
AIC	Akaike Information Criterion
AIE	average intensity of exposure
AIHA	American Industrial Hygiene Association
ALB	albumin
ALDH	aldehyde dehydrogenase
ALL	acute lymphocytic leukemia
ALM	anterior lateral meatus
ALP	alkaline phosphatase
ALS	amyotrophic lateral sclerosis
ALT	alanine aminotransferase
AML	acute myelogenous leukemia
AMM	anterior medial maxilloturbinate
AMPase	adenosine monophosphatase
AMS	anterior medial septum
ANAE	alpha-naphthylacetate esterase
ANOVA	analysis of variance
APA	American Psychiatric Association
ARB	Air Resources Board
AST	aspartate aminotransferase
ATCM	airborne toxic control measure
ATP	adenosine triphosphate
ATPase	adenosine triphosphatase
ATS	American Thoracic Society
ATSDR	Agency for Toxic Substances and Disease Registry
AUC	area under the curve
BAL	bronchoalveolar lavage
BALT	bronchus associated lymphoid tissue
BBDR	biologically based dose response
BC	bronchial construction
BCME	bis(chloromethyl)ether
BDNF	brain-derived neurotrophic factor
BEIR	biologic effects of ionizing radiation
BfR	German Federal Institute for Risk Assessment
BHR	bronchial hyperresponsiveness
BMC	benchmark concentration
BMCL	95% lower bound on the benchmark concentration
BMCR	binuclated micronucleated cell ratefluoresce
BMD	benchmark dose
BMDL	95% lower bound on the benchmark dose

BMR	benchmark response
BN	Brown-Norway
BrdU	bromodeoxyuridine
BUN	blood urea nitrogen
BW	body weight
CA	chromosomal aberrations
CalEPA	California Environmental Protection Agency
CAP	College of American Pathologists
CASRN	Chemical Abstracts Service Registry Number
CAT	catalase
CBMA	cytokinesis-blocked micronucleus assay
CBMN	cytokinesis-blocked micronucleus
CDC	U.S. Centers for Disease Control and Prevention
CDHS	California Department of Health Services
CFD	computational fluid dynamics
CGM	clonal growth model
CHO	Chinese hamster ovary
CI	confidence interval
CIIT	Chemical Industry Institute of Toxicology
CLL	chronic lymphocytic leukemia
CML	chronic myelogenous leukemia
CNS	central nervous system
CO_2	carbon dioxide
COEHHA	California Office of Environmental Health Hazard Assessment
CREB	cyclic AMP responsive element binding proteins
CS	conditioned stimulus
$C \times t$	concentration times time
DA	Daltons
DAF	dosimetric adjustment factor
DDX	DNA-DNA cross-links
DEI	daily exposure index
DEN	diethylnitrosamine
Der f	common dust mite allergen
DMG	dimethylglycine
DMGDH	dimethylglycine dehydrogenase
DNA	deoxyribonucleic acid
DOPAC	3,4-dihydroxyphenylacetic acid
DPC / DPX	DNA-protein cross-links
EBV	Epstein-Barr virus
EC	effective concentration
ED	effective dose
EHC	Environmental Health Committee
ELISA	enzyme-linked immunosorbent assay

LIST OF ABBREVIATIONS AND ACRONYMS (continued)

EPA	U.S. Environmental Protection Agency
ERPG	emergency response planning guideline
ET	ethmoid turbinates
FALDH	formaldehyde dehydrogenase
FDA	U.S. Food and Drug Administration
FDR	fecundability density ratio
FEF	forced expiratory flow
FEMA	Federal Emergency Management Agency
FEV1	forced expiratory volume in 1 second
FISH	fluorescent in situ hybridization
FSH	follicle-stimulating hormone
FVC	forced vital capacity
GALT	gut-associated lymphoid tissue
GC-MS	gas chromatography-mass spectrometry
GD	gestation day
GI	gastrointestinal
GO	gene ontology
G6PDH	glucose-6-phosphate dehydrogenase
GPX	glutathione peroxidase
GR	glutathione reductase
GM-CSF	granulocyte macrophage-colony-stimulating factor
GSH	reduced glutathione
GSNO	S-nitrosoglutathione
GST	glutathione S-transferase
HAP	hazardous air pollutant
Hb	hemoglobin
HCl	hydrochloric acid
HCT	hematocrit
HEC	human equivalent concentration
5-HIAA	5-hydroxyindoleacetic acid
hm	hydroxymethyl
HMGSH	S-hydroxymethylglutathione
HPA	hypothalamic-pituitary adrenal
HPG	hypothalamo-pituitary-gonadal
HPLC	high-performance liquid chromatography
HPRT	hypoxanthine-guanine phosphoribosyl transferase
HR	high responders
HSA	human serum albumin
HSDB	Hazardous Substances Data Bank
Hsp	heat shock protein
HWE	healthy worker effect
I cell	initiated cell
IARC	International Agency for Research on Cancer

LIST OF ABBREVIATIONS AND ACRONYMS (continued)

ICD	International Classification of Diseases
IF	interfacial
IFN	interferon
Ig	immunoglobulin
IL	interleukin
I.P.	intraperitoneal
IPCS	International Programme on Chemical Safety
IRIS	Integrated Risk Information System
K_m	Michaels-Menton constant
KM	Kaplan-Meier
LD_{50}	median lethal dose
LDH	lactate dehydrogenase
LEC	95% lower bound on the effective concentration
LED	95% lower bound on the effective dose
LHP	lymphohematopoietic
LI	labeling index
LM	Listeria monocytogenes
LMS	linearized multistage
LLNA	local lymph node assay
LOAEL	lowest-observed-adverse-effect level
LPS	lipopolysaccharide
LR	low responders
LRT	lower respiratory tract
MA	methylamine
MALT	mucus-associated lymph tissues
MCH	mean corpuscular hemoglobin
MCHC	mean corpuscular hemoglobin concentration
MCS	multiple chemical sensitivity
MCV	mean corpuscular volume
MDA	malondialdehyde
MEF	maximal expiratory flow
ML	myeloid leukemia
MLE	maximum likelihood estimate
MMS	methyl methane sulfonate
MMT	medial maxilloturbinate
MN	micronucleus, micronuclei
MNNG	N-methyl-N-nitro-N-nitrosoguanidine
MOA	mode of action
MoDC	monocyte-derived dendritic cell
MP	macrophage
MPD	multistage polynomial degree
MPS	mononuclear phagocyte system
MRL	minimum risk level

LIST OF ABBREVIATIONS AND ACRONYMS (continued)

mRNA	messenger ribonucleic acid
MVE-2	Murray Valley encephalitis virus
MVK	Moolgavkar, Venzon, and Knudson
N cell	normal cell
NaCl	sodium choride
NAD+	nicotinamide adenine dinucleotide
NADH	reduced nicotinamide adenine dinucleotide
NALT	nasally associated lymphoid tissue
NATA	National-Scale Air Toxics Assessment
NCEA	National Center for Environmental Assessment
NCHS	National Center for Health Statistics
NCI	National Cancer Institute
NEG	Nordic Expert Group
NER	nucleotide excision repair
NGF	nerve growth factor
NHL	non-Hodgkin's lymphoma
NHMRC/ARMCANZ	National Health and Medical Research Council/Agriculture and Resource Management Council of Australia and New Zealand
NNK	nitrosamine nitrosamine 4-(methylnitrosamino)-1-(3-pyridyl)-butanone
N^6-hmdA	N^6-hydroxymethyldeoxyadenosine
N^4-hmdC	N^4-hydroxymethylcytidine
N^2-hmdG	N^2-hydroxymethyldeoxyguanosine
NICNAS	National Industrial Chemicals Notification and Assessment Scheme
NIOSH	National Institute for Occupational Safety and Health
NLM	National Library of Medicine
NMDA	N-methyl-D-aspartate
NO	nitric oxide
NOAEL	no-observed-adverse-effect level
NPC	nasopharyngeal cancer
NRBA	neutrophil respiratory burst activity
NRC	National Research Council
NTP	National Toxicology Program
OR	odds ratio
OSHA	Occupational Safety and Health Administration
OTS	Office of Toxic Substances
OVA	ovalbumin
PBPK	physiologically based pharmacokinetic
PC	Philadelphia chromosome
PCA	passive cutaneous anaphylaxis
PCMR	proportionate cancer mortality ratio
PCNA	proliferating cell nuclear antigen
PCR	polymerase chain reaction
PCV	packed cell volume

LIST OF ABBREVIATIONS AND ACRONYMS (continued)

PECAM	platelet endothelial cell adhesion molecule
PEF	peak expiratory flow
PEFR	peak expiratory flow rates
PEL	permissible exposure limit
PFC	plaque-forming cell
PG	periglomerular
PHA	phytohemagglutinin
PLA2	phospholipase A2
PI	phagocytic index
PLM	posterior lateral meatus
PMA	phorbol 12-myristate 13-acetate
PMR	proportionate mortality ratio
PMS	posterior medial septum
PND	postnatal day
POD	point of departure
POE	portal of entry
PTZ	pentilenetetrazole
PUFA	polyunsaturated fatty acids
PWULLI	population weighted unit length labeling index
RA	reflex apnea
RANTES	regulated upon activation, normal T–cell expressed and secreted
RB	reflex bradypnea
RBC	red blood cells
RD_{50}	exposure concentration that results in a 50% reduction in respiratory rate
REL	recommended exposure limit
RfC	reference concentration
RfD	reference dose
RGD	regional gas dose
RGDR	regional gas dose ratio
RR	relative risk
RT	reverse transcriptase
SAB	Science Advisory Board
SCC	squamous cell carcinoma
SCE	sister chromatid exchange
SCG	sodium cromoglycate
SD	standard deviation
SDH	succinate dehydrogenase; sarcosine dehydrogenase
SEER	Surveillance, Epidemiology, and End Results
SEM	standard error of the mean
SEN	sensitizer
SH	sulfhydryl
SHE	Syrian hamster embryo
SLMA	spontaneous locomotor activity

LIST OF ABBREVIATIONS AND ACRONYMS (continued)

SMR	standardized mortality ratio
SNP	single nucleotide polymorphism
SOD	superoxide dismutase
SOMedA	N^6-sulfomethyldeoxyadenosine
Sp1	specificity protein
SPIR	standardized proportionate incidence ratio
SSAO	semicarbozole-sensitive amine oxidase
SSB	single strand breaks
STEL	short-term exposure limit
TBA	tumor bearing animal
TH	T-lymphocyte helper
THF	tetrahydrofolate
TK	toxicokinetics
TL	tail length
TLV	threshold limit value
TNF	tumor necrosis factor
TP	total protein
TRI	Toxic Release Inventory
TRPV	transient receptor potential vanilloid
TWA	time-weighted average
TZCA	thiazolidine-4-carboxylate
UCL	upper confidence limit
UDS	unscheduled DNA synthesis
UF	uncertainty factor
UFFI	urea formaldehyde foam insulation
ULLI	unit length labeling index
URT	upper respiratory tract
USDA	U.S. Department of Agriculture
VC	vital capacity
VOC	volatile organic compound
WBC	white blood cell
WDS	wet dog shake
WHO	World Health Organization
WHOROE	World Health Organization Regional Office for Europe

FOREWORD

The purpose of this Toxicological Review is to provide scientific support and rationale for the hazard and dose-response assessment in IRIS pertaining to chronic inhalation exposure to formaldehyde. It is not intended to be a comprehensive treatise on the chemical or toxicological nature of formaldehyde.

In Chapter 6, *Major Conclusions in the Characterization of Hazard and Dose Response,* EPA has characterized its overall confidence in the qualitative and quantitative aspects of hazard and dose response by addressing knowledge gaps, uncertainties, quality of data, and scientific controversies. The discussion is intended to convey the limitations of the assessment and to aid and guide the risk assessor in the ensuing steps of the risk assessment process.

For other general information about this assessment or other questions relating to IRIS, the reader is referred to EPA's IRIS Hotline at (202) 566-1676 (phone), (202) 566-1749 (fax), or hotline.iris@epa.gov (email address).

AUTHORS, CONTRIBUTORS, AND REVIEWERS

CHEMICAL MANAGERS

John E. Whalan, D.A.B.T.[1]
EPA-ORD-NCEA

Danielle DeVoney, PhD, D.A.B.T., PE[2]
EPA-ORD-NCEA

AUTHORS

Thomas Bateson, PhD
EPA-ORD-NCEA

Susan Euling, PhD
EPA-ORD-NCEA

Jennifer Jinot, PhD

Susan Makris, PhD
EPA-ORD-NCEA

Kathleen Raffaele, PhD
EPA-ORD-NCEA

John Schaum, PhD
EPA-ORD-NCEA

Ravi Subramaniam, PhD
EPA-ORD-NCEA

Suryanarayana Vulimiri, PhD
EPA-ORD-NCEA

CONTRIBUTORS

Gillian Backus, PhD [3]

Stanley Barone, PhD
EPA-ORD-NCEA

---

[1] Chemical Manager since July 2003.
[2] Chemical Manager since June 2009
[3] Separated from the Agency prior to final revisions to document.

AUTHORS, CONTRIBUTORS, AND REVIEWERS (continued)

David Bayliss, PhD [3]
EPA-ORD-NCEA

Ted Berner, PhD
EPA-ORD-NCEA

David Bussard
EPA-ORD-NCEA

David Farrar, PhD
EPA-ORD-NCEA

John Fox, PhD
EPA-ORD-NCEA
EPA-ORD-NCEA

Karen Hogan, PhD
EPA-ORD-NCEA

Rosemarie Hakim, PhD [3]
EPA-ORD-NCEA

Babashaheb Sonawane, PhD
EPA-ORD-NCEA

Chad Thompson, PhD [3]
EPA-ORD-NCEA

Larry Valcovic, PhD [3]
EPA-ORD-NCEA

John J. Vandenberg, PhD
EPA-ORD-NCEA

Lisa Vinikoor, PhD
EPA-ORD-NCEA

Paul White, PhD
EPA-ORD-NCEA

CONTRACTOR SUPPORT

The literature search and preliminary drafts of this document as well as support for editing and formatting were provided by Oak Ridge Institute for Science and Education (ORISE), Oak Ridge Associated Universities (ORAU), Department of Energy, under Interagency Agreement (IAG) Project No. 03-18. The ORISE individuals who contributed to this effort include Sheri Hester, George Holdsworth, Bobette D. Nourse, Wanda Olson, and Lutz W. Weber.

Assistance with the biologically based dose response model evaluation was provided by ENVIRON International Corporation of Monroe, Louisiana (subcontractors to ORISE; Project No. 03-18). The primary scientists involved in the work were Kenny S. Crump and Cynthia Van Landingham.

INTERNAL EPA REVIEWERS

Daniel Axelrad, PhD
Office of Policy, Economics, and Innovation

Iris Camacho, PhD
Office of Pollution Prevention and Toxics

Christina Cinalli, PhD
Office of Pollution Prevention and Toxics

Rebecca Edelstein, PhD
Office of Pollution Prevention and Toxics

Ernest Falke, PhD
Office of Pollution Prevention and Toxics

Stiven Foster, PhD
Office of Solid Waste and Emergency Response

Greg Fritz
Office of Pollution Prevention and Toxics

Susan Griffin, PhD
EPA Region 8

AUTHORS, CONTRIBUTORS, AND REVIEWERS (continued)

Timothy Leighton, PhD
Office of Pesticide Programs

Elizabeth Margosches, PhD
Office of Pollution Prevention and Toxics

Timothy McMahon, PhD
Office of Pesticde Programs

Julie Migrin-Sturza, PhD
Office of Policy, Economics, and Innovation

Greg Miller, PhD
Office of Children’s Health Protection and Environmental Education

Deirdre Murphy, PhD
Office of Air and Radiation

Marion Olson, PhD
EPA Region 2

Andrea Pfahles-Hutchens, PhD
Office of Pollution Prevention and Toxics

Jennifer Seed, PhD
Office of Pollution Prevention and Toxics

This page intentionally left blank.

1. INTRODUCTION

This document presents background information and justification for the Integrated Risk Information System (IRIS) Summary of the hazard and dose-response assessment of formaldehyde. IRIS Summaries may include oral reference dose (RfD) and inhalation reference concentration (RfC) values for chronic and other exposure durations, and a carcinogenicity assessment.

The RfD and RfC, if derived, provide quantitative information for use in risk assessments for health effects known or assumed to be produced through a nonlinear (presumed threshold) mode of action. The RfD (expressed in units of mg/kg-day) is defined as an estimate (with uncertainty spanning perhaps an order of magnitude) of a daily exposure to the human population (including sensitive subgroups) that is likely to be without an appreciable risk of deleterious effects during a lifetime. The inhalation RfC (expressed in units of mg/m^3) is analogous to the oral RfD, but provides a continuous inhalation exposure estimate. The inhalation RfC considers toxic effects for both the respiratory system (portal of entry [POE]) and for effects peripheral to the respiratory system (extrarespiratory or systemic effects). Reference values are generally derived for chronic exposures (up to a lifetime), but may also be derived for acute (≤24 hours), short-term (>24 hours up to 30 days), and subchronic (>30 days up to 10% of lifetime) exposure durations, all of which are derived based on an assumption of continuous exposure throughout the duration specified. Unless specified otherwise, the RfD and RfC are derived for chronic exposure duration.

The carcinogenicity assessment provides information on the carcinogenic hazard potential of the substance in question and quantitative estimates of risk from oral and inhalation exposure may be derived. The information includes a weight-of-evidence judgment of the likelihood that the agent is a human carcinogen and the conditions under which the carcinogenic effects may be expressed. Quantitative risk estimates may be derived from the application of a low-dose extrapolation procedure. If derived, the oral slope factor is a plausible upper bound on the estimate of risk per mg/kg-day of oral exposure. Similarly, an inhalation unit risk is a plausible upper bound on the estimate of risk per $\mu g/m^3$ air breathed.

Development of these hazard identification and dose-response assessments for formaldehyde has followed the general guidelines for risk assessment as set forth by the National Research Council (NRC) (1983). EPA Guidelines and Risk Assessment Forum Technical Panel Reports that may have been used in the development of this assessment include the following: *Guidelines for the Health Risk Assessment of Chemical Mixtures* (U.S. EPA, 1986a), *Guidelines for Mutagenicity Risk Assessment* (U.S. EPA, 1986b), *Recommendations for and Documentation* *of Biological Values for Use in Risk Assessment* (U.S. EPA, 1988), *Guidelines for Developmental Toxicity Risk Assessment* (U.S. EPA, 1991), *Interim Policy for Particle Size and Limit Concentration Issues in Inhalation Toxicity* (U.S. EPA, 1994a), *Methods for Derivation of Inhalation Reference Concentrations and Application of Inhalation Dosimetry* (U.S. EPA, 1994b), *Use of the Benchmark Dose Approach in Health Risk Assessment* (U.S. EPA, 1995), *Guidelines for Reproductive Toxicity Risk Assessment* (U.S. EPA, 1996), *Guidelines for Neurotoxicity Risk Assessment* (U.S. EPA, 1998), *Science Policy Council Handbook*: *Risk Characterization* (U.S. EPA, 2000a), *Benchmark Dose Technical Guidance Document* (U.S. EPA, 2000b), *Supplementary Guidance for Conducting Health Risk Assessment of Chemical Mixtures* (U.S. EPA, 2000c), *A Review of the Reference Dose and Reference Concentration Processes* (U.S. EPA, 2002a), *Guidelines for Carcinogen Risk Assessment* (U.S. EPA, 2005a), *Supplemental Guidance for Assessing Susceptibility from Early-Life Exposure to Carcinogens* (U.S. EPA, 2005b), *Science Policy Council Handbook*: *Peer Review* (U.S. EPA, 2006a), and *A Framework for Assessing Health Risks of Environmental Exposures to Children* (U.S. EPA, 2006b).

The literature search strategy employed for this compound was based on the Chemical Abstracts Service Registry Number (CASRN) and at least one common name. Any pertinent scientific information submitted by the public to the IRIS Submission Desk was also considered in the development of this document. The relevant literature was reviewed through April, 2009, but some criticial literature after this date has been considered in this assessment.

2. BACKGROUND

This chapter provides an overview of the physical and chemical characteristics of formaldehyde. Also provided in this chapter are a description of the production, uses, and sources of formaldehyde and information regarding environmental levels and human exposure. A description of the toxicokinetics and toxicodynamic processes involved in formaldehyde toxicity for the inhalation, oral, and dermal routes can be found in Chapter 3 (Toxicokinetics).

2.1. PHYSICOCHEMICAL PROPERTIES OF FORMALDEHYDE

Formaldehyde (CASRN 50-00-0) is the first of the series of aliphatic aldehydes and is a gas at room temperature. Its molecular structure is depicted in Figure 2-1. It is noted for its reactivity and versatility as a chemical intermediate. It readily undergoes polymerization, is highly flammable, and can form explosive mixtures with air. It decomposes at temperatures above 150°C.

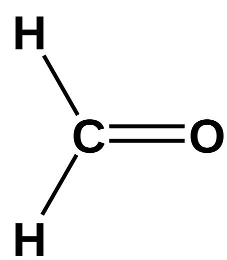

Figure 2-1. Chemical structure of formaldehyde.

At room temperature, pure formaldehyde is a colorless gas with a strong, pungent, suffocating, and highly irritating odor. Formaldehyde is readily soluble in water, alcohols, ether, and other polar solvents. A synopsis of its physicochemical properties is given in Table 2-1.

2.2. PRODUCTION, USES, AND SOURCES OF FORMALDEHYDE

Formaldehyde has been produced commercially since the early 1900s and, in recent years, has been ranked in the top 25 highest volume chemicals produced in the U.S. (National Toxicology Program [NTP], 2002). In 2003, 4.33 million metric tons of formaldehyde were produced in the U.S. (Global Insight, 2006). In 2000, worldwide formaldehyde production was estimated to be 21.5 million metric tons, (International Agency for Research on Cancer [IARC], 2006).

Table 2-1. Physicochemical properties of formaldehyde

Name	Formaldehyde
International Union for Pure and Applied Chemistry name	Formaldehyde
Synonyms	Formic aldehyde Methanal Methyl aldehyde Methylene oxide Oxomethane Oxymethylene
Chemical Abstracts Service Index name	Formaldehyde
CASRN	50-00-0
Formula	HCHO
Molecular weight	30.03
Density	Gas: 1.067 (air = 1) Liquid: 0.815 g/mL at –20°C
Vapor pressure	3,883 mm Hg at 25°C
Log K_{ow}	–0.75 to 0.35
Henry's law constant	3.4×10^{-7} atm-m^3/mol at 25°C 2.2×10^{-2} Pa-m^3/mol at 25°C
Conversion factors (25°C, 760 mm Hg)	1 ppm = 1.23 mg/m^3 (v/v) 1 mg/m^3 = 0.81 ppm (v/v)
Boiling point	–19.5°C at 760 mm Hg
Melting point	–92°C
Flash point	60°C; 83°C, closed cup for 37 %, methanol-free aqueous solution; 50°C closed cup for 37% aqueous solution with 15% methanol
Explosive limits	73% upper; 7% lower by volume in air
Autoignition temperature	300°C
Solubility	Very soluble in water; soluble in alcohols, ether, acetone, benzene
Reactivity	Reacts with alkalis, acids and oxidizers

Sources: American Conference of Governmental Industrial Hygienists (ACGIH) (2002); International Programme on Chemical Safety (IPCS) (2002); Agency for Toxic Substances and Disease Registry (ATSDR) (1999); Gerberich and Seaman (1994); Walker (1975).

Formaldehyde is a chemical intermediate used in the production of plywood adhesives, abrasive materials, insulation, foundry binders, brake linings made from phenolic resins, surface coatings, molding compounds, laminates, wood adhesives made from melamine resins, phenolic thermosetting, resin curing agents, explosives made from hexamethylenetetramine, urethanes, lubricants, alkyd resins, acrylates made from trimethylolpropane, plumbing components from polyacetal resins, and controlled-release fertilizers made from urea formaldehyde concentrates

(IPCS, 1989). Formaldehyde is used in smaller quantities for the preservation and embalming of biological specimens. It is also used as a germicide, an insecticide, and a fungicide, as well as an antimicrobial agent in soaps, shampoos, hair preparations, deodorants, lotions (e.g., suntan lotion and dry skin lotion), makeup, and mouthwashes, and is present in hand cream, bath products, mascara and other eye makeup, cuticle softeners, nail creams, vaginal deodorants, and shaving cream (IPCS, 2002; ATSDR, 1999).

Formaldehyde is commonly produced as an aqueous solution called formalin, which usually contains about 37% formaldehyde and 12–15% methanol. Methanol is added to formalin to slow polymerization that leads eventually to precipitation as paraformaldehyde. Paraformaldehyde has the formula $(CH_2O)_n$ where n is 8 to 100. It is essentially a solid form of formaldehyde and therefore has some of the same uses as formaldehyde (Kiernan, 2000). When heated, paraformaldehyde sublimes as formaldehyde gas. This characteristic makes it useful as a fumigant, disinfectant, and fungicide, such as for the decontamination of laboratories, agricultural premises, and barbering equipment. Long-chain polymers (e.g., Delrin plastic) are less inclined to release formaldehyde, but they have a formaldehyde odor and require additives to prevent decomposition (U.S. EPA, 2008).

The major sources of anthropogenic emissions of formaldehyde are motor vehicle exhaust, power plants, manufacturing plants that produce or use formaldehyde or substances that contain formaldehyde (i.e., adhesives), petroleum refineries, coking operations, incineration, wood burning, and tobacco smoke. Among these anthropogenic sources, the greatest volume source of formaldehyde is automotive exhaust from engines not fitted with catalytic converters (NEG, 2003). The Toxic Release Inventory (TRI) data for 2007 show total releases of 21.9 million pounds with about half to the air and half to underground injection (EPA TRI Explorer, http://www.epa.gov/triexplorer/) (U.S. EPA, 2009a).

Formaldehyde is formed naturally in the lower atmosphere during the oxidation of hydrocarbons (i.e., methane and terpene), which react with hydroxyl radicals and ozone to form formaldehyde and other aldehydes, as intermediates in a series of reactions that ultimately lead to the formation of carbon monoxide and carbon dioxide, hydrogen and water. Formaldehyde can also be formed in a variety of other natural processes, such as decomposition of plant residues in the soil, photochemical processes in sea water, and forest fires (National Library of Medicine [NLM], 2001).

Formaldehyde emitted to the ambient air primarily reacts with photochemically generated hydroxyl radicals in the troposphere or undergoes direct photolysis (IPCS, 2002). Overall, half-lives for formaldehyde in air can vary considerably under different conditions. Estimates for atmospheric residence time in several U.S. cities ranged from 0.3 hours under conditions typical of a rainy winter night to 250 hours under conditions typical of a clear summer night (assuming no reaction with hydroperoxyl radicals). Given the generally short daytime residence times for formaldehyde, there is limited potential for long-range transport (IPCS, 2002). In cases where organic precursors are transported long distances, however, secondary formation of formaldehyde may occur far from the anthropogenic sources of the precursors.

Formaldehyde is released to water from the discharges of both treated and untreated industrial wastewater from its production and from its use in the manufacture of formaldehyde-containing resins (ATSDR, 1999). Formaldehyde is also a possible drinking-water disinfection by-product from the use of ozone and/or hydrogen peroxide. In water, formaldehyde is rapidly hydrated to form a glycol, and the equilibrium favors the glycol.

2.3. ENVIRONMENTAL LEVELS AND HUMAN EXPOSURE

General population exposure to formaldehyde can occur via inhalation, ingestion and dermal contact. Each of these pathways and associated media levels are discussed below. Formaldehyde exposure can also occur occupationally via three main scenarios:

- The production of aqueous solutions of formaldehyde (formalin) and their use in the chemical industry (e.g., for the synthesis of various resins, as a preservative in medical laboratories and embalming fluids, and as a disinfectant).
- Release from formaldehyde-based resins in which it is present as a residue and/or through their hydrolysis and decomposition by heat (e.g., during the manufacture of wood products, textiles, synthetic vitreous insulation products, and plastics). In general, the use of phenol–formaldehyde resins results in much lower emissions of formaldehyde than those of urea- based resins.
- The pyrolysis or combustion of organic matter (e.g., in engine exhaust gases or during firefighting) (IARC, 2006).

Industries with the greatest potential for exposure include health services, business services, printing and publishing, manufacture of chemicals and allied products, manufacture of apparel and allied products, manufacture of paper and allied products, personal services, machinery (except clerical), transport equipment, and furniture and fixtures (IARC, 1995).

2.3.1. Inhalation

The most current ambient air monitoring data for formaldehyde come from EPA's air quality system database (EPA's AirData Web site: http://www.epa.gov/air/data/index.html) (U.S. EPA, 2009b). These data have been collected from a wide variety of sources, including state and local environmental agencies, but have not been collected from a statistically based survey. The most recent data, for the year 2007, come from 188 monitors located in 33 states as shown in Figure 2-2 (U.S. EPA, 2008). The annual means for these monitors range from 0.7–45.03 μg/m^3 (0.56–36.31 ppb) and have an overall average of 3.44 μg/m^3 (2.77 ppb). The annual means are derived by EPA by averaging all available daily data from each monitor. Table 2-2 shows a breakout of the data by land use category based on the annual means from each monitor for 2005, 2006, and 2007. The land use is established on the basis of the most prevalent land use within 0.25 miles of the monitor. The mobile category (land near major highways or interstates such that it is primarily impacted by mobile sources) has the highest mean levels, and agricultural lands have the lowest.

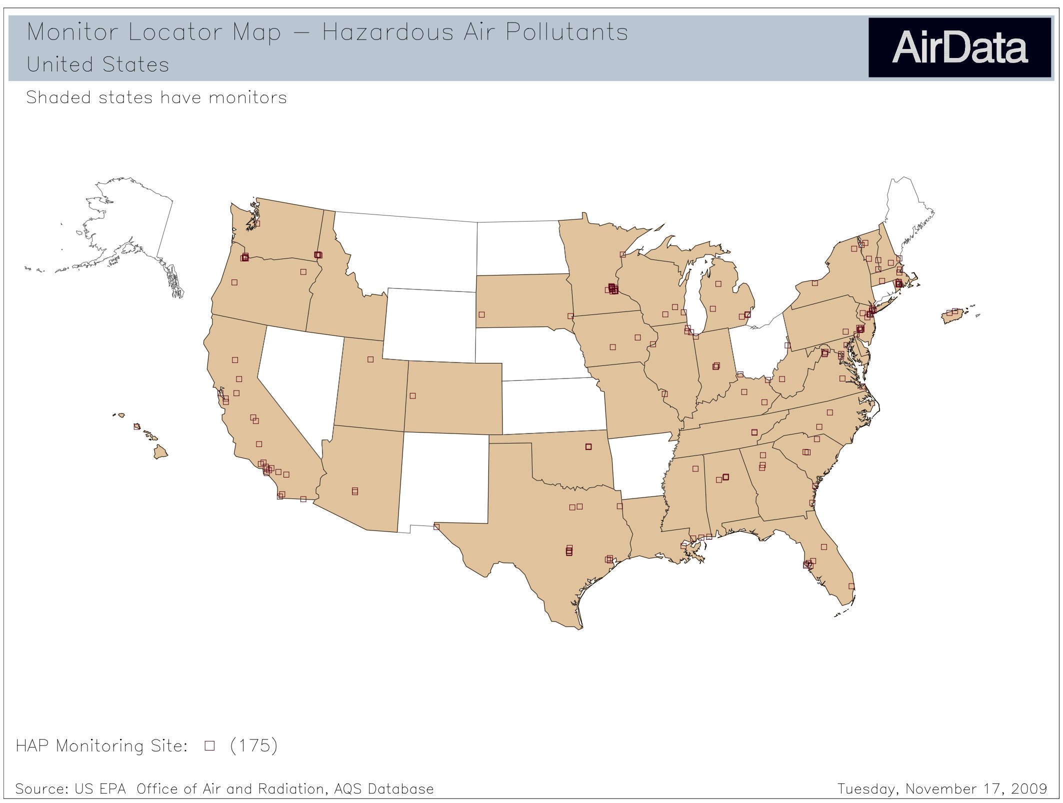

Figure 2-2. Locations of hazardous air pollutant monitors.

Dasgupta et al. (2005) measured formaldehyde levels in 5 U.S. cities during 1999 - 2002. Samples were collected over approximately a one month period in the spring or summer. Mean levels were 5.05 ppb in Nashville, TN; 7.96 ppb in Atlanta, GA; 4.49 ppb in Houston, TX; 3.12 ppb in Philadelphia, PA; and 2.63 in Sydney, FL.

Table 2-2. Ambient air levels by land use category

	Formaldehyde Exposure by Category[a]					
	Agriculture	**Commercial**	**Forest**	**Industrial**	**Mobile**[b]	**Residential**
Number of data points	17	166	19	61	16	282
Mean ± standard deviation	2.08 ± 0.98	3.26 ± 2.76	2.79 ± 2.17	6.28 ± 14.45	6.84 ± 7.28	2.75 ± 1.71
Minimum	0.34	0.20	0.40	0.14	2.02	0.17
Maximum	4.34	20.61	7.33	74.72	23.39	12.35

[a]Values are µg/m^3.
[b]"Mobile" is ambient air in locations primarily impacted by mobile sources.

Source: AirData for 2005, 2006, and 2007 (U.S. EPA, 2009b).

Under the National-Scale Air Toxics Assessment (NATA) program, EPA has conducted an emissions inventory for a variety of hazardous air pollutants (HAPs), including formaldehyde (U.S. EPA, 2006c). The NATA uses the emissions inventory data to model nationwide air concentrations/exposures (U.S. EPA, 2006c). The results of the 1999 ambient air concentration modeling for formaldehyde suggest that county median air levels range from 0 to 6.94 µg/m^3 (0 – 5.59 ppb) with a national median of 0.56 µg/m^3 (0.45 ppb) (see Figure 2-3). Similar results were found for the year 2002: county concentrations ranged from 0.12 to 9.17 µg/m^3 (0.097 – 7.38 ppb) with median of 0.78 µg/m^3 (0.63 ppb). NATA has not provided updated concentration maps for 2002. The 1999 map shows the highest levels in the far west and northeastern regions of the U.S. While these modeling results can be useful, it is important to consider their limitations. Some of the geographical differences result from differences in methods used by states supplying the data. For example, the high levels indicated for Idaho result from the large amount of wood burned during forest fires and the relatively high emission factor that Idaho uses (compared with other states) to estimate formaldehyde emissions from forest fires. A comparison of modeling results from NATA to measured values at the same locations is presented in U.S. EPA (2006c). For 1999, it was found that formaldehyde levels were underestimated at 76% of the sites (n = 68). One possible reason why the NATA results appear low compared to measurements is that the modeling has not accounted for secondary formation of formaldehyde in the atmosphere.

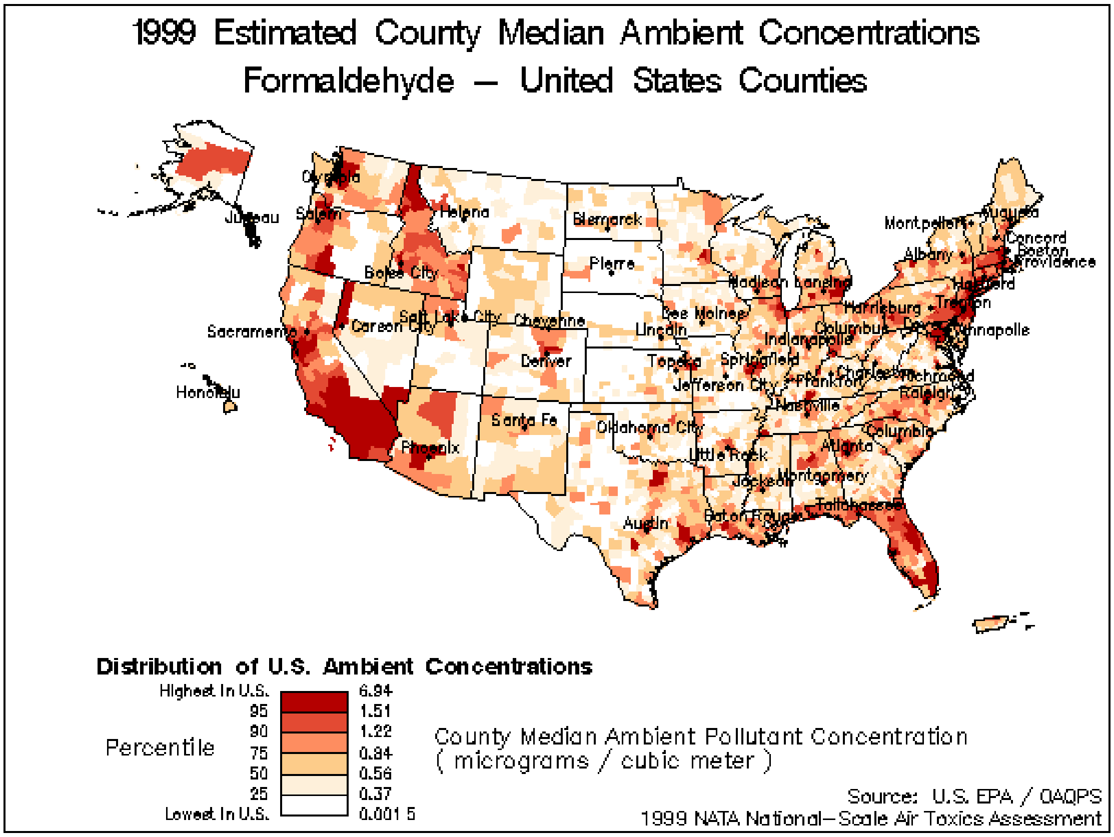

Figure 2-3. Modeled ambient air concentrations based on 1999 emissions.

In general, ambient levels of formaldehyde in outdoor air are significantly lower than those measured in the indoor air of workplaces or residences (ATSDR, 1999; IARC, 1995). Indoor sources of formaldehyde in air include volatilization from pressed wood products, carpets, fabrics, insulation, permanent press clothing, latex paint, and paper bags, along with emissions from gas burners, kerosene heaters, and cigarettes (NLM, 2001). In general, the major indoor air sources of formaldehyde can be described in two ways: 1) those sources that have the highest emissions when the product is new with decreasing emission over time, as with the first set in the examples above; and 2) those sources that are reoccurring or frequent such as the second set of examples above. Gilbert et al. (2006) studied 96 homes in Quebec City, Canada and found elevated levels in homes with new wood or melamine furniture purchased within the previous 12 months. A summary of indoor data is provided in Table 2-3. Results vary depending on housing characteristics and date of study.

Table 2-3. Studies on residential indoor air levels of formaldehyde (non-occupational)

Citation	No. of Samples	Target Population/House Type	Mean (µg/m^3)	Range (µg/m^3)
Gold et al., 1993		Complaint homes Older conventional homes	<60	24 - 960
Hare et al., 1996		Newly built homes	91	
Hare et al., 1996		30 days after installing pressed wood	42 - 540	
Gammage and Hawthorne, 1985	>1200 131 >500 260	Homes with UFFI Homes without UFFI Complaint mobile homes Newer mobile homes Older mobile homes	60 - 144 30 - 84 120 - 1080 1032 300	12 - 4080 12 - 204 0 - 5040
Hawthorne et al., 1986 a,b	18 11 11 40	Conventional homes 0-5 yr Conventional homes 5-15 yr Conventional homes >15 yr Conventional homes overall	96 48 36 72	 24 - 480
U.S.EPA, 1987	560	Noncomplaint, conventional, randomly selected Noncomplaint, mobile homes, randomly selected	32-109 109-744	6-576 12-3480
Health Canada and Environment Canada, 2001	151	Residential (Canadian) noncomplaint homes	35	?-148
Zhang et al., 1994 a,b	6	Residential, carpeted, non-smoking homes	66	42-89
Gilbert et al., 2006	96	Residential (Canadian)	29.5	9.6 – 90.0
Shah and Singh, 1988	315	Residential & commercial	59	23-89
Stock, 1987	43	Conventional homes	84	96-216
Krzyzanowski et al., 1990	202	Conventional homes	31	

Note: 1 ppb = 1.2 µg/m^3

Salthammer et al. (2010) present a thorough review of formaldehyde sources and levels found in the indoor environment. Based on an examination of international studies carried out in 2005 or later they conclude that the average exposure of the population to formaldehyde is 20 to 40 μg/m^3 under normal living conditions. They used the diagram shown in Figure 2-4 to summarize data they found on the range of formaldehyde air concentrations (in ppb) in different environments.

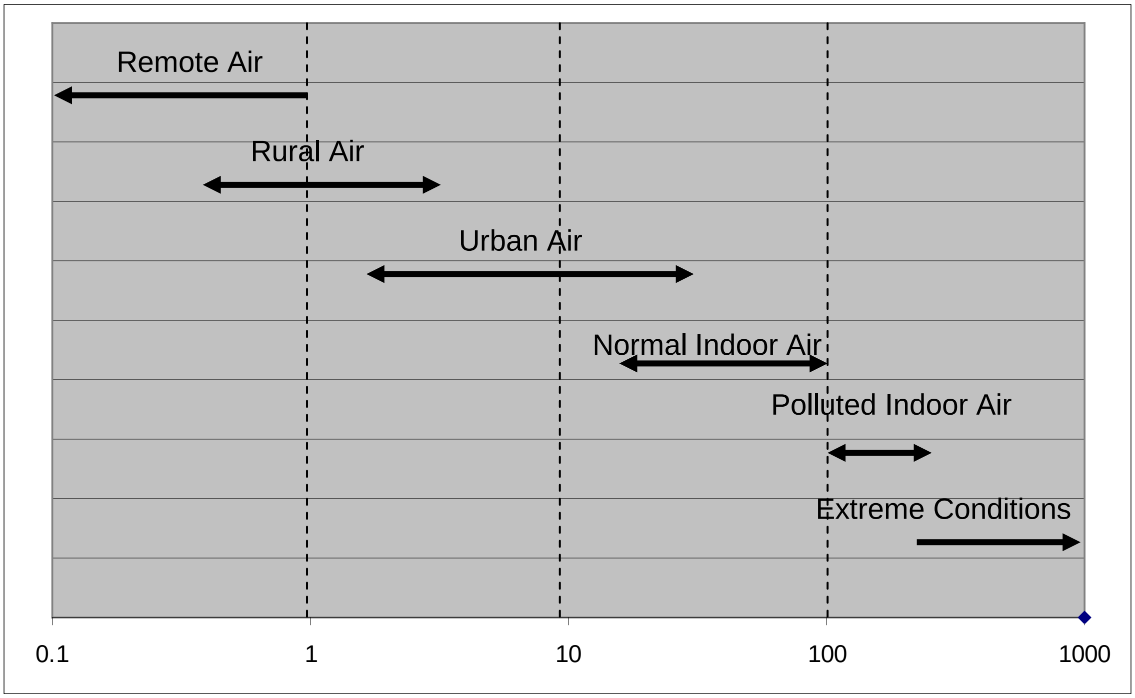

Figure 2-4. Range of formaldehyde air concentrations (ppb) in different environments. Source: Salthammer et al. (2010)

Data on formaldehyde levels in outdoor and indoor air were collected under Canada's National Air Pollution Surveillance program (IPCS, 2002; Health Canada and Environment Canada, 2001). The effort included four suburban and four urban sites sampled in the period 1990–1998. A Monte Carlo analysis applied to the pooled data (n = 151) was used to estimate the distribution of time-weighted 24-hour air exposures. This study suggested that mean levels in outdoor air were 3.3 μg/m^3 (2.7 ppb) and mean levels in indoor air were 35.9 μg/m^3 (29.2 ppb) (Health Canada and Environment Canada, 2001). The simulation analysis also suggested that general population exposures averaged 33–36 μg/m^3 (27–30 ppb).

Since the early to mid 1980s, manufacturing processes and construction practices have been changed to reduce levels of indoor formaldehyde emissions (ATSDR, 1999). A 2008 law enacted by the California Air Resource Board (CARB. 2008, Final Regulation Order: Airborne Toxic Control Measure to Reduce Formaldehyde Emissions from Composite Wood Products; http://www.arb.ca.gov/regact/2007/compwood07/fro-final.pdf) has limited the amount of formaldehyde that can be released by specific composite wood products (i.e., hardwood plywood, particle board, and medium density fiberboard) sold, supplied, or manufactured for use in California. For this reason the mean indoor air levels presented by Health Canada and Environment Canada (2001) (based on samples collected from 1989–1995) may overestimate current levels. In addition, the Canadian indoor air data may overestimate formaldehyde levels in U.S. homes, because many residential homes in Canada use wood burning stoves more frequently and have tighter construction (due to colder winters), leading to less dilution of indoor emissions. The outdoor air levels, however, appear to have remained fairly constant over recent years, and the median outdoor level from the Canadian study (2.8 $\mu g/m^3$) (2.3 ppb) is very similar to the median of the U.S. monitoring data (2.83 $\mu g/m^3$) (2.3 ppb) in 1999.

Even though formaldehyde levels in construction materials have declined, indoor inhalation concerns still persist. For example, recent studies have measured formaldehyde levels in mobile homes. ATSDR (2007) reported on air sampling in 96 unoccupied trailers provided by the Federal Emergency Management Agency (FEMA) used as temporary housing for people displaced by Hurricane Katrina. Formaldehyde levels in closed trailers averaged 1,250 ± 828 $\mu g/m^3$ (mean ± standard deviation [SD]) (1.04 ± 0.69 ppm), with a range of 12–4,390 $\mu g/m^3$ (0.01–3.66 ppm). The levels decreased to an average of 468 ± 324 $\mu g/m^3$ (0.39 ± 0.27 ppm), with a range of 0.00–1,960 $\mu g/m^3$ (0.00–1.63 ppm) when the air conditioning was turned on. Levels also decreased to an average of 108 ± 96 $\mu g/m^3$ (0.09 ± 0.08 ppm), with a range of 12–588 $\mu g/m^3$ (0.01–0.49 ppm) when the windows were opened. ATSDR (2007) found an association between temperature and formaldehyde levels; higher temperatures were associated with higher formaldehyde levels in trailers with the windows closed. They also noted that different commercial brands of trailers yielded different formaldehyde levels.

In December 2007 and January 2008, the Centers for Disease Control and Prevention (CDC) measured formaldehyde levels in a stratified random sample of 519 FEMA-supplied occupied travel trailers, park models, and mobile homes ("trailers") (CDC, 2008). At the time of the study, sampled trailers were in use as temporary shelters for Louisiana and Mississippi residents displaced by hurricanes Katrina and Rita. The geometric mean level of formaldehyde in sampled trailers was 95 $\mu g/m^3$ (77 ppb), and the range was 3.7–730 $\mu g/m^3$ (3–590 ppb).

2.3.2. Ingestion

Limited U.S. data indicate that concentrations in drinking water may range up to approximately 10 μg/L in the absence of specific contributions from the formation of formaldehyde by ozonation during water treatment or from leaching of formaldehyde from polyacetyl plumbing fixtures (IPCS, 2002). In the absence of other data, one-half this concentration (5 μg/L) was judged to be a reasonable estimate of the average formaldehyde in

Canadian drinking water. Concentrations approaching 100 μg/L were observed in a U.S. study assessing the leaching of formaldehyde from domestic polyacetal plumbing fixtures, and this concentration was assumed to be representative of a reasonable worst case (IPCS, 2002).

Formaldehyde is a natural component of a variety of foodstuffs (IARC, 1995; IPCS, 1989). However, foods may be contaminated with formaldehyde as a result of fumigation (e.g., grain fumigation), cooking (as a combustion product), and release from formaldehyde resin-based tableware (IARC, 1995). Also, the compound has been used as a bacteriostatic agent in some foods, such as cheese (IARC, 1995). There have been no systematic investigations of levels of formaldehyde in a range of foodstuffs that could serve as a basis for estimation of population exposure (Health Canada and Environment Canada, 2001). According to the limited available data, concentrations of formaldehyde in food are highly variable. In the few studies of the formaldehyde content of foods in Canada, the concentrations were within a range of <0.03–14 mg/kg (Health Canada and Environment Canada, 2001). Data on formaldehyde levels in food have been presented by Feron et al. (1991) and IPCS (1989) from a variety of studies, yielding the following ranges of measured values:

- Fruits and vegetables: 3–60 mg/kg
- Meat and fish: 6–20 mg/kg
- Shellfish: 1–100 mg/kg
- Milk and milk products: 1–3.3 mg/kg

Daily intake of formaldehyde was estimated by IPCS (1989) to be in the range of 1.5–14 mg for an average adult. Similarly, Fishbein (1992) estimated that the intake of formaldehyde from food is 1–10 mg/day but discounted this on the belief that it is not available in free form. Although the bioavailability of formaldehyde from the ingestion of food is not known, it is not expected to be significant (ATSDR, 1999). Using U.S. Department of Agriculture (USDA) (1979) consumption rate data for various food groups, Owen et al. (1990) calculated that annual consumption of dietary formaldehyde results in an intake of about 4,000 mg or approximately 11 mg/day.

2.3.3. Dermal Contact

The general population may have dermal contact with formaldehyde-containing materials, such as some paper products, fabrics, and cosmetics. For example, nail hardeners contain formalin, and cosmetics products such as hand creams and suntan lotions contain formaldehyde-releasing agents (but not formaldehyde) as preservatives. Generally, though, dermal contact is more of a concern in occupations that involve handling concentrated forms of formaldehyde, such as those occurring in embalming and chemical production.

3. TOXICOKINETICS

3.1. CHEMICAL PROPERTIES AND REACTIVITY

Formaldehyde (HCHO) is the smallest aldehyde (30 g/mol) and is a gas at room temperature. It is highly water soluble and reactive. In water, less than 0.1% of formaldehyde exists unhydrated, with the majority reported to be in the hydrated form, methylene glycol ($CH_2(OH)_2$) (Priha et al., 1996). Formaldehyde reacts readily with high and low molecular weight biological constituents.

3.1.1. Binding of Formaldehyde to Proteins

Formaldehyde is a reactive molecule that is likely to react with both low molecular weight cellular components (e.g., reduced glutathione[GSH]) as well as high molecular weight components. Unlike deoxyribonucleic acid (DNA), which has some additional barriers to exposure (i.e., nucleus), extracellular and intracellular proteins are obvious targets for interacting with formaldehyde. Formaldehyde is a well-known cross-linking agent that is used in the fixation of tissues, preparation of vaccines, and study of protein-protein interactions (Metz et al., 2006). However, the exact nature of the protein modifications used for these purposes is not yet fully characterized (Metz et al., 2006, 2004). Figure 3-1 provides a general reaction scheme for formaldehyde-mediated modifications of amino acids. In step 1, formaldehyde reacts with primary N-terminal amines to form a labile methylol adduct. This adduct can undergo dehydration (step 2) to form an imine, or Schiff base ($-N{=}CH_2$). Metz et al. (2004) examined the types of formaldehyde-protein reactions that are likely to occur in vivo by synthesizing several identical polypeptides with one varying amino acid (X) within the sequence VEL**X**VLL (V=valine, E=glutamate, L=Leucine, X=varying amino acid). Several peptides with reactive amino acids did not exhibit modifications, suggesting that the peptide sequence/structure affects the ability of formaldehyde to react with amino acids. Peptides that were modified indicated formation of methylol adducts (Figure 3-1, step 1) or a mixture of methylol and imine adducts (Figure 3-1, step 2).

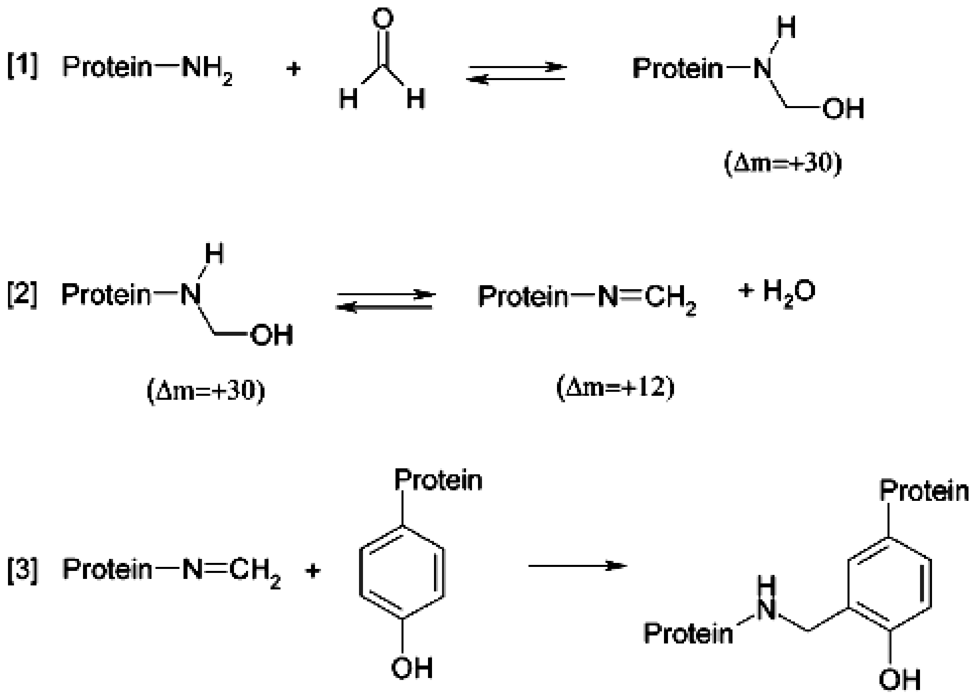

Figure 3-1. Formaldehyde-mediated protein modifications.

Note: Formaldehyde reacts with primary *N*-terminal amines to form a methylol adduct [1], which increases the molecular weight by 30 Da (Δm). This labile adduct can rearrange to form an amine, or Schiff base [2], that results in an increase in MW of 12 Da. Schiff bases can react with certain amino acids to form intra- or intermolecular methylene bridges [3]. The two amino acids depicted in step 3 may be within the same protein or possibly from two different proteins.

Source: Metz et al. (2004).

Mucus is composed of water, electrolytes, polysaccharides, and about 0.5% soluble proteins (Priha et al., 1996; Bogdanffy et al., 1987). Bogdanffy et al. (1987) showed that although human nasal mucus can bind 70% of 100 mM formaldehyde, irreversible binding of [^{14}C]-formaldehyde to serum albumin (the major protein in mucus) was shown to be insignificant after a 1-hour incubation. Irreversible binding (50% or more) did not occur until after about 7 hours of incubation. These data suggest that the protein content of mucus may not provide a significant formaldehyde irreversible sink. Nonetheless, the solubility of formaldehyde in mucus along with mucus flow and ingestion likely indicate that much of the inhaled dose is removed—perhaps as much as 42% in rodents (IARC, 2005; Schlosser, 1999).

In general, formaldehyde interacts with proteins. Studies carried out in cell culture media containing serum and formaldehyde have shown that such mixtures are quite labile. For example, during a 60-minute incubation of formaldehyde with complete cell media (i.e., with fetal calf serum) at 38°C, gas chromatography-mass spectrometry (GC-MS) exhibited very different peak profiles at different points during the incubation (Proctor et al., 1986). In contrast, GC-MS chromatograms of cell media containing formaldehyde but no serum proteins appeared relatively unchanged throughout the incubation. Compared to cell culture medium alone, complete media were considered to provide a more suitable model for the hypothetical interactions that formaldehyde could undergo in vivo (including perhaps blood).

3.1.2. Endogenous Sources of Formaldehyde

Endogenous formaldehyde is produced through a) normal cellular metabolism through enzymatic or non-enzymatic reactions, and also as a detoxification product of xenobiotics during cellular metabolism:

3.1.2.1. *Normal Cellular Metabolism (Enzymatic)*

Formaldehyde is produced during normal metabolism of methanol, amino acids (e.g., glycine, serine, methionine), choline, dimethylglycine, and methylamine and through the folate-dependent endogenous one-carbon pool etc.

i) One of the endogenous sources for formaldehyde production is methanol, formed during normal cellular metabolism. However, this fraction may also be derived through consumption of fruits, vegetables and alcohol (Shelby et al . 2004; IPCS, 1997). In studies conducted with healthy humans whose diet was devoid of methanol-containing or methanol-generating foods (such as cereals containing aspartame, a precursor of methanol) and who abstained from alcohol consumption, the background blood levels of methanol range from 0.25–4.7 mg/L (Reviewed in Shelby et al 2004 [CERHR]). Methanol is metabolized to formaldehyde predominantly by hepatic alcohol dehydrogenase-1 (ADH1) in primates and by ADH1 and catalase (CAT) in rodents, ADH1 requiring nicotinamide adenine dinucleotide (NAD^+) as a cofactor.

ii) Dimethylglycine (DMG), one of the byproducts of choline metabolism endogenously present in the body, is an indirect source of endogenous formaldehyde. Two specific dehydrogenases, i) dimethylglycine dehydrogenase (DMGDH) which converts DMG to sarcosine (methylglycine) and ii) sarcosine dehydrogenase (SDH) which converts sarcosine to glycine, have been shown to non-covalently bind to the folate enzyme, tetrahydrofolate (THF). Further, these dehydrogenases form "active formaldehyde" by removing the 1-carbon groups from THF (Binzak et al., 2000).

iii) Another source of endogenous formaldehyde is methylamine (MA), an intermediary component of the metabolism of adrenaline, sarcosine, creatine, lecithin, and other dietary sources (Yu and Zuo 1996). The enzyme semicarbozole-sensitive amine oxidase (SSAO), predominantly present in the plasma membrane of endothelial smooth muscle cells and in circulating blood, converts methylamine to formaldehyde, hydrogen peroxide and ammonia. The formaldehyde thus released has been shown to cause endothelial injury eventually leading to atherosclerosis (Kalasz, 2003). Yu et al. (1997) have shown that adrenaline, released in the body as a response to stress, is known to be deaminated by the enzyme monoamine oxidase, with further conversion of methylamine to formaldehyde by SSAO (Yu et al . 1997). Creatine is another precursor for methylamine which is metabolized by SSAO to form formaldehyde. It has been shown that short-term, high-dose dietary supplementation of creatine in healthy humans causes a significant increase in urinary methylamine and formaldehyde levels (Poortmans et al., 2005).

iv) Endogenous formaldehyde is also a constituent of the one-carbon pool, a network of interrelated biochemical reactions that involve the transfer of one-carbon groups from one compound to another (usually the transfer of the hydroxymethyl group of serine to tetrahydrofolic acid).

Tyihak et al. (1998) have demonstrated that formaldehyde, but not the methyl radical or methyl cation, is involved in the enzymatic transmethylation and demethylation reactions, and suggested the presence of a formaldehyde cycle in cells for the production and removal of formaldehyde utilizing the transfer through methionine → S-adenosylmethionine → S-adenosyl-homocysteine → homocysteine (Tyihak et al., 1998). However, these studies did not clearly show whether the formaldehyde released in this cycle is in free or bound form.

Formaldehyde has been shown to be produced in normal and leukemic leukocytes from N^5-methyl-THF by enzymatic degradation (Thorndike and Beck, 1977). This is a two-step reaction involving 1) enzymatic conversion of the methyl-THF to formaldehyde followed by 2) nonenzymatic reaction of formaldehyde with an amine. Thorndike and Beck (1977) showed that leukocyte (granulocyte and lymphocyte) cell extracts from normal individuals and patients with chronic lymphocytic leukemia (CLL) or chronic myelocytic leukemia (CML) incubated with ^{14}C-methyl-THF and saturating amounts of tryptamine produced free formaldehyde which is detected as its corresponding carboline derivative formed with tryptamine. These results demonstrate the activity of the enzyme N^5, N^{10}-methylene THF reductase which oxidizes N^5-methyltetrahydrofolate to N^5, N^{10} methylene THF. The authors noted that the enzyme levels were in the order of normal granulocytes < normal lymphocytes < granulocytes from a CML individual < lymphocytes from a CLL individual (Thorndike and Beck, 1977), suggesting increased activity of formaldehyde producing enzyme in leukemic cells compared to normal leukocytes. Overall, formaldehyde might be a byproduct as well as an intermediary product in several of these reactions.

3.1.2.2. *Normal Metabolism (Non-Enzymatic)*

i) Formaldehyde can also be formed non-enzymatically by the spontaneous reaction of methanol with hydroxyl radicals, wherein cellular hydrogen peroxide is the precursor for hydroxyl radicals generated through Fenton reaction (Cederbaum and Qureshi, 1982).

ii) Another mechanism of nonenzymatic production of formaldehyde is through lipid peroxidation of polyunsaturated fatty acids (PUFA) (Shibamoto, 2006; Slater, 1984). In this mechanism, reactive oxygen species (ROS) generated during oxidative stress abstract a hydrogen atom from a methylene group of polyunsaturated fatty acids (PUFA) in cell membranes causing autooxidation of lipids with the eventual production of free radicals (e.g., peroxy radical). It is known that a certain level of oxidative stress and lipid peroxidation does occur in normal individuals, and these cellular metabolic processes are likely to contribute to endogenous formaldehyde production.

3.1.2.3. *Exogenous Sources of Formaldehyde Production*

Microsomal cytochrome P450 enzymes catalyze oxidative demethylation of N-, O- and S-methyl groups of xenobiotic compounds whereby formaldehyde is produced as a primary product, which is subsequently incorporated into the one-carbon pool by reacting with tetrahydrofolic acid or is oxidized to formate (Dahl and Hadley, 1983; Heck et al., 1982). Also, some special peroxidases, such as peroxide-dependent horseradish peroxidase enzymatically catalyze xenobiotics to generate formaldehyde in the body. In particular, an ethyl peroxide-dependent horseradish peroxidase has been shown to act on *N*,*N*-dimethylaniline and produce equimolar amounts of *N*-methylaniline and formaldehyde (Kedderis and Hollenberg, 1983). The tobacco-specific nitrosamine nitrosamine 4-(methylnitrosamino)-1-(3-pyridyl)-butanone (NNK) is another source of formaldehyde. It has been shown that formaldehyde is also produced during the methyl hydroxylation of NNK by rat liver microsomes (Castonguay et al., 1991). Also recent studies have demonstrated the formation of formaldehyde-DNA adducts in

NNK-treated rats using a highly sensitive liquid chromatography-electrospray ionization-tandem mass spectrometry with selected reaction monitoring (Wang et al., 2007), suggesting formation of formaldehyde from nitrosamines. Cigarette smoke is also a source of exogenously produced methylamine which is converted to formaldehyde by SSAO (Yu, 1998).

3.1.2.4. *FA-GSH Conjugate as a Method of Systemic Distribution*

Formaldehyde is primarily metabolized by alcohol dehydrogenase (ADH3) which uses the formaldehyde-glutathione hemiacetal adduct as the substrate. Sanghani et al. (2000) have shown that due to high circulating concentrations (50-fold) of glutathione in human blood, the S-(hydroxymethyl)glutathione (HMGSH) adduct, the nonenzymatic product of formaldehyde with glutathione is the major form of formaldehyde seen in vivo (Sanghani et al., 2000). It is likely that the reversibly bound HMGSH may be transported to different tissues through circulation, but, specific experimental evidence is lacking.

3.1.2.5. *Metabolic Products of FA Metabolism (e.g., Formic Acid)*

Formate is converted to carbon dioxide (CO_2) in rodents predominantly by a folate-dependent enzyme pathway (Dikalova et al., 2001). Formate is also oxidized to CO_2 and water by a minor pathway involving catalase located in rat liver peroxisomes (Waydhas et al., 1978; Oshino et al., 1973). In the folate-dependent pathway, tetrahydrofolate (THF)-mediated oxidation of formate and the transfer of one-carbon compounds between different derivatives of THF has been described.

Endogenous levels of formate also will be affected by dietary intake of methanol-producing or methanol-containing diets since methanol is initially converted to formaldehyde and eventually metabolized to formate. It has been shown in several studies in human subjects who were restricted on consuming methanol producing diets, aspartame or alcohol, that the endogenous blood concentrations of formate ranged from 3.8 to 19.1 mg/L (Shelby et al 2004 [CERHR]). The biological half life of formic acid is 77-90 min (Owen et al., 1990b). The levels of formate in the urine of unexposed individuals range from 11.7 to 18 mg/L (Boeniger, 1987). One source of formic acid intake is through diet which ranges from 0.4 to 1.2 mg per day (Boeniger 1987). The half life for plasma formate is ~30 minutes or longer (Boeniger 1987).

3.1.2.6. *Levels of Endogenous Formaldehyde in Animal and Human Tissues*

Heck et al. (1982) estimated that endogenous levels of formaldehyde (free as well as bound) in rats ranged from 0.05 to 0.5 µmole/g (1.5-15 µg/g) of wet tissue as analyzed by the stable isotope dilution with GC-MS method (Heck et al., 1982). Although the levels of free formaldehyde cannot be measured due to their high reactivity and short half life, they were calculated by Heck et al. (1985) using an indirect method. They added a molar excess of GSH or THF to the test tube containing formaldehyde in aqueous solution enabling complete binding. When estimated, they observed that the amount of formaldehyde detected was equal to the total amount added to the reaction suggesting that the formaldehyde measured contained both free and bound forms. Further, they calculated the free formaldehyde concentration using the dissociation constant of the HMGSH adduct and cellular concentration of GSH. Human formaldehyde dehydrogenase has been shown to have a dissociation constant of 1.5 mM for the formaldehyde-GSH hemithioacetal adduct (Uotila and Koivusalo 1974), while the folate enzyme product N^5,N^{10}-methylene-THF has a dissociation constant of 30 mM (Kallen and Jencks 1966b; a). This could be evaluated using the Michaels-Menton constant (K_m) of formaldehyde dehydrogenase for the GSH adduct (~4 µM at 25^{o}C), whereby they calculated the free formaldehyde level to be around 3-7 µM or 1-2% of the total formaldehyde as measured by GC-MS in rat tissues (Heck 1982).

Cascieri and Clary (1992) estimated the total body content of formaldehyde in human body based on the following assumptions. For an individual with an average body wt of 70 kg and with body fluids accounting for 70% of body weight, total formaldehyde content is distributed in ~49 kg of body mass or 49 L of body fluids, owing to the water solubility and uniform distribution of formaldehyde in body fluids. It has been shown that the average blood concentration (mean ± S.E.) of formaldehyde in unexposed rats and humans was 2.24 ± 0.07 and 2.61 ± 0.14 µg/g of blood, respectively (Heck et al., 1985), and in unexposed rhesus monkeys it was 2.42 ± 0.09 µg/g of blood (Casanova et al., 1988), overall giving an average of approximately 2.5 ppm (2.5 mg/L) formaldehyde across the species. All these studies used pentafluorophenyl hydrazine derived formaldehyde using GC-MS analysis (Table 3-1). Assuming these values, the body content of total formaldehyde is 122.5 mg (49 L x 2.5 mg/L) or 1.75 mg/kg body wt at any given time. Formaldehyde given intravenously to rhesus monkeys has been shown to have a half life of ~1.5 min in blood, wherein formaldehyde in blood was measured by the dimedone method (McMartin et al., 1979). Using this information Cascieri and Clary (1992) calculated that the human body generates approximately 40.83 mg/min [(122.5 mg /2 x 1.5] of formaldehyde. Biotransformation of formaldehyde to carbon dioxide in the liver alone has been estimated at 22 mg/minute (Owen et al., 1990a).

Free formaldehyde is detected in body fluids and tissues using dimedone (Szarvas et al., 1986) or 2,4-dinitrohenyhydrazine (DNPH) or pentafluoropheyl hydrazine (PFPH) derivative (Heck et al., 1985) or as a fluorescent derivative (Luo et al . 2001) as trapping agent and detected by analytical techniques such as thin-layer chromatography (TLC), high-performance liquid chromatography (HPLC) and gas-chromatography mass spectrometry (GC-MS). Data from several studies is summarized in Table 3-1. Using ^{14}C-labeled dimedone, a chemical which condenses with free formaldehyde forming a product termed "formaldemethone" enabling radiometric detection, Szarvas et al (1986) estimated the levels of endogenous formaldehyde in human blood plasma to be 0.4-0.6 µg/mL and in human urine to be 2.5-4 µg/mL (Szarvas et al . 1986).

Table 3-1. Endogenous formaldehyde levels in animal and human tissues and body fluids

Tissue	Method	Detected as	Formaldehyde levels	Reference
Not specified	Not specified	Not specified	0.003-0.012 ppm (3-12 ng/g)	Hileman 1984
Not specified	GC-MS with stable isotope dilution method	As PFPH-derivative	1.5 - 15 ppm (0.05-0.5 µmole/g)	Heck et al 1982a
Blood	GC-MS with select ion monitoring	As PFPH-derivative	2.24 ± 0.07 ppm (2.24 ± 0.07 µg/g)	Heck et al 1985
Blood	GC-MS with select ion monitoring	As PFPH-derivative	2.61 ± 0.14 ppm (2.61 ± 0.14 µg/g)	Heck et al 1985
Plasma	Reverse phase HPLC-fluorescent detection	As product of ampicillin	1.65 ppm (1.65 µg/mL)	Luo et al 2001
Heart perfusate	HPLC	As DNPH adduct	0.089 - 0.126 ppm (2.98 - 4.21 nmol/mL)	Shibamoto 2006
Blood	GC-MS with select ion monitoring	As PFPH-derivative	2.42 ± 0.09 ppm (2.42 ± 0.09 µg/g)	Casanova et al 1988
Plasma	Radiometric method	As formalde-methone adduct	0.4 - 0.6 ppm (0.4 - 0.6 µg/mL)	Szarvas et al 1986
Urine	Radiometric method	As formalde-methone adduct	2.5 - 4.0 ppm (2.5 - 4.0 µg/mL)	Szarvas et al 1986

Values in the parenthesis, originally cited in the references, are converted to parts per million (ppm) as indicated. PFPH, pentafluorophenyl hydrazone derivative; DNPH, dinitrophenyl hydrazine; GC-MS, gas-chromatography mass spectrometry; HPLC, high performance liquid chromatography.

Hileman (1984) reported that the endogenous levels of metabolically derived formaldehyde will be in the range of 3-12 ng/g of tissue (Hileman 1984). So for an average 70 kg individual, the endogenous level of metabolically derived formaldehyde would be 210 µg to 840 µg (3-12 ng/g x 1000 g x 70).

3.2. ABSORPTION

3.2.1. Oral

Oral absorption of [^{14}C]-formaldehyde (7 mg/kg) in rats resulted in 40% elimination as ^{14}C-carbon dioxide ($^{14}CO_2$), with 10% excretion in urine, 1% excretion in feces, and much of the remaining 49% retained within the carcass, presumably due to metabolic incorporation (IARC, 1995; Buss et al., 1964).

3.2.2. Dermal

Jeffcoat et al. (1983) reported on the disposition of various doses of [^{14}C]-formaldehyde dermally administered to rats, guinea pigs, and monkeys. Very little (<1% of the applied dose) of the radiolabel was found in the major organs excised during necropsy. As noted by the authors, the disposition of formaldehyde when administered via the dermal route was markedly different to that observed when the compound was administered intravenously or intraperitoneally. In the latter cases, there was much evidence of metabolic activity, and substantial portions of the load were expired as CO_2. The difference appeared to be the result of a reaction of dermally applied formaldehyde with macromolecules at or near the skin surface or of its evaporation. In general, portions of the load that succeed in entering the circulation probably do so bound to macromolecules or by incorporation of the radiolabel via the one-carbon pool. Likewise, Bartnik et al. (1985) who applied [^{14}C]-formaldehyde to the shaved backs of rats concluded that the overwhelming majority of the formaldehyde load remained sequestered in the outer layers of skin at or near the site of application. At the end of the various measurements, approximately 70% of the dose was found in the treated skin, with a marked localization of the remaining radioactivity in the uppermost layers. This fraction of the load was considered to be permanently sequestered, most likely as a result of irreversible binding to macromolecular components.

3.2.3. Inhalation

Studies indicate that the majority of inhaled formaldehyde is absorbed in the upper respiratory tract (URT) but that the extent of the scrubbing in this region varies significantly across species. In dogs, nearly 100% of nasally inhaled formaldehyde is absorbed (Egle, Jr., 1972). Lower respiratory tract (LRT) studies designed to collect formaldehyde via a tube inserted into the lower trachea revealed that nearly 95% of formaldehyde was absorbed during the first pass through the upper respiratory tract (Egle, Jr., 1972), an effect observed with multiple ventilation rates. The rat nasal passages also scrub nearly all of the inhaled formaldehyde (on average ~97%) (Morgan et al., 1986). In computational dosimetry modeling based on anatomically realistic representation of the human nasal airways from a single individual, approximately 90% of inhaled formaldehyde was predicted to be absorbed in the nose at resting inspiration. As the inspiratory rate increased, this fraction decreased to about 70% at light exercise and to 58% at heavy exercise conditions (see Figure 1 in Kimbell et al. [2001b]). The normal human breathing mode during heavy exercise is oronasal (with ~54% of airflow being oral) (ICRP 66, 1994). Consequently, it is estimated that during heavy exercise breathing (50 L/min) the flux of formaldehyde into tissue (or rate of mass transported per mm^2 of tissue surface area) in the first six to eight generations of the tracheobronchial airways is comparable to that in the nasal region (Overton et al., 2001).

It is important to note that the computer simulations mentioned above are based on anatomical representations of a single individual. Significant anatomical variations occur in human nasal airways. For example, the nasal volumes of 10 adult nonsmoking subjects between 18 and 50 years of age in a study in the U.S. varied between 15 and 60 mL (Santiago et al., 2001), and disease states can result in considerable further variation (Singh et al., 1998).

Species differences in kinetic factors have been argued to be the key determinants of species-specific lesion distributions for formaldehyde and other reactive inhaled gases. Airway geometry is an important determinant of inhaled-formaldehyde dosimetry in the respiratory tract and its differences across species. These issues will be discussed in a later section on dosimetry modeling.

3.2.3.1. *Formaldehyde Uptake Can Be Affected by Effects at the Portal of Entry*

Certain formaldehyde-related effects have the potential to modulate its uptake and clearance. The mucociliary apparatus of the upper respiratory tract is the first line of defense against airborne toxins. Comprising a thick mucus layer (epiphase), hydrophase, and a ciliated epithelium, the mucociliary apparatus may entrain, neutralize, and remove particulates and airborne chemicals from inspired air. As reviewed by Wolfe (1986), airborne pollutants and reactive gases have been shown to decrease mucus flow rates in several animal models (Mannix et al., 1983; Iravani, 1974; Carson et al., 1966; Dalhamn, 1956; Cralley, 1942). Degradation in the continuity or function of this mucociliary apparatus could result in a lower clearance of inhaled pollutants at the portal of entry.

Morgan et al. (1983) first reported defects in mucociliary function in F344 rats exposed to 15 ppm formaldehyde 6 hours/day for 1–9 days. Mucostasis occurred in several regions in all rats after a single 15 ppm exposure. Ciliastasis occurred with greater frequency and across more regions of the nasoturbinate in subsequent days of exposure. The authors observed that mucostasis preceded ciliastasis in most cases, and vigorous ciliary activity was noted in areas without mucus flow. Morgan et al. (1984a) also studied formaldehyde effects on the mucociliary apparatus of isolated frog palates in vitro. Mucostasis was evident as mucus became stiff and eventually rigid with increasing formaldehyde concentration and time of exposure. Ciliary beat continued even after mucostasis, but ciliastasis ultimately occurred when exposure reached 4 and 9 ppm.

When a rodent is exposed to an irritant, its inhaled dose and pattern of deposition can be profoundly affected by reflex bradypnea, a protective reflex seen in rodents but not in humans. Reflex bradypnea can occur when the trigeminal nerve is exposed to a sufficient concentration of an irritant, such as formaldehyde. It is manifest as markedly decreased activity or prostration, reduced metabolism, hypothermia (as much as 5ºC), significantly reduced respiratory rate and minute volume, and altered blood and brain chemistry. Because of their small size, rodents are able to rapidly lower their metabolism and body temperature and therefore their oxygen demand. The consequence is that their inhaled dose of an irritating chemical is dramatically lowered. Reflex bradypnea is quantified as the RD_{50}, which is the concentration of a chemical that results in a 50% decrease in respiratory rate. It can take as much as two hours for rodents to fully recover from the effects of reflex bradypnea. The clinical manifestations of reflex bradypnea can easily be misconstrued as toxicity. None of the studies described in this assessment took into account the fact that reflex bradypnea may have confounded the results. Reflex bradypnea is discussed in depth in section 4.2.1.1.

Sensory irritation studies suggest that formaldehyde activates the trigeminal nerve by activating nociceptors through the modification of receptor amino acids, possibly including thiol groups. Cassee et al. (1996) measured sensory irritation to formaldehyde, acetaldehyde, and acrolein in male Wistar rats, following a 30-minute nose-only exposure. Formaldehyde and acrolein elicited similar responses, whereas acetaldehyde was far less irritating. The authors suggested that the differences in sensitivity to the aldehydes might be explained by differences in physicochemical properties and by regional differences in activities of detoxifying enzymes for each chemical. In addition, it has been suggested that acetaldehyde might interact with sensory nerves via an amino group (Steinhagen and Barrow, 1984), whereas the receptor-binding site for formaldehyde and acrolein is believed to be a thiol group. Differential binding sites for sensory irritants in the trigeminal nerve have been reported (Nielsen, 1991).

Sensory irritation effects are discussed in depth in Chapter 4 but are noted here because stimulation of the trigeminal nerve by formaldehyde can result in significantly lower pulmonary ventilation, and formaldehyde exposure in rodents at concentrations that approach the RD_{50}. Barrow et al. (1983) have estimated the “inhaled dose” equivalent to an exposure concentration of 15 ppm in mice and rats used in the chronic formaldehyde bioassays by Kerns et al. (1983)

and Monticello and Morgan (1994). Their results indicate that, because mice are observed to decrease their minute volume by approximately 75% as compared to 45% in rats, a twofold greater inhaled dose would be expected in rats versus mice. This difference may be relevant to the increased incidence of squamous cell carcinoma of the nasal cavity in F344 rats as compared to B6C3F1 mice. Chang et al. (1983) estimated a reduction of 25% in the minute volume of F344 rats. Yokley et al. (2008) have recently published a model that accounts for physiological changes in ventilation rate induced by sensory irritation in rats. Thus, the “standard” minute volumes used for rats and mice need to be adjusted downward when calculating dosimetric adjustment factors for extrapolation of adverse effects to humans (Thompson et al., 2008). This question is further discussed in the section on modeling the dosimetry.

Another effect that modulates dosimetry is the dynamic tissue remodeling of nasal airways that occurs as a consequence of exposure to reactive gases. For example, formaldehyde dosimetry is influenced by the occurrence of squamous metaplasia, an adaptive tissue conversion to squamous that occurs in nasal epithelium exposed to toxic levels of formaldehyde. The metaplasia has been observed to occur in rats at exposure concentrations of 3 ppm and higher (Kimbell et al., 1997). Squamous epithelium is known to absorb considerably less formaldehyde than other epithelial types (Kimbell et al., 1997). Overall, the highest flux levels of formaldehyde in the simulations of the rat nose in Kimbell et al. (2001a) are estimated in the region just posterior to the nasal vestibule. A consequence of squamous metaplasia would be to “push” the higher levels of formaldehyde flux toward the more distal regions of the nose (Kimbell et al., 1997). Subramaniam et al. (2008) discussed this issue further in the context of uncertainties in the modeling of formaldehyde dosimetry.

3.2.3.2. *Variability in the Nasal Dosimetry of Formaldehyde in Adults and Children*

Garcia et al. (2009) used computational fluid dynamics to study human variability in the nasal dosimetry of reactive, water-soluble gases in 5 adults and 2 children, aged 7 and 8 years old. They considered two model categories of gases, corresponding to maximal and moderate absorption at the nasal lining. We focus here only on the “maximum uptake” simulations in Garcia et al. (2009). In this case, the gas was considered so highly reactive and soluble that it was reasonable to assume an infinitely fast reaction of the absorbed gas with compounds in the airway lining. Although such a gas could be reasonably considered to represent formaldehyde, these results cannot be fully utilized to inform quantitative estimates of formaldehyde dosimetry (and it does not appear to have been the intent of the authors either). This is because the same boundary condition corresponding to maximal uptake was applied on the vestibular lining of the nose as well as on the transitional and transitional epithelial lining on the rest of the nose. This is not appropriate for formaldehyde as the lining on the nasal vestibule is made of keratinized epithelium which is considerably less absorbing than the rest of the nose (Kimbell et al. 2001).

The Garcia et al. (2009) study and the results of their analyses have been further described and evaluated in Appendix 3-1. Overall uptake efficiency, average flux (rate of gas absorbed per unit surface area of the nasal lining) and maximum flux levels over the entire nasal lining did not vary substantially between adults (1.6-fold difference in average flux and much less in maximum flux), and the mean values of these quantities were comparable between adults and children. These results are in agreement with conclusions reached by Ginsberg et al. (2005) that overall extrathoracic absorption of highly and moderately reactive and soluble gases (corresponding to category 1 and 2 reactive gases as per the scheme in USEPA [1994]) is similar in adults and children. On the other hand, Figure 6A of the paper (reproduced as Figure A in Appendix 3-1), shows significant interhuman variability in flux values at specific points on the nasal walls. The local flux of formaldehyde varies among individuals by a factor of 3 to 5 at various distances along the septal axis of the nose.

3.3. DISTRIBUTION

3.3.1. Levels in Blood

Inhalation studies in several species indicate that exposure to formaldehyde does not result in elevated levels in blood. These studies were carried out over a wide range of exposure concentrations and durations. Rats exposed to 14 ppm formaldehyde for 2 hours exhibited no increase in blood formaldehyde levels [2.25 ± 0.07 μg/(g blood) in treated animals compared with 2.24 ± 0.07 μg/(g blood) in control animals] when measured by GC-MS using a stable isotope dilution technique (Heck et al., 1985, 1982). Similarly, mean formaldehyde blood levels in humans (n = 6) exposed to 1.9 ppm formaldehyde for 40 minutes in a walk-in chamber (2.77 ± 0.28 μg/g blood) were not statistically different from measurements in the same population before exposure (mean of 2.61 ± 0.14 μg/g) (Heck and Casanova-Schmitz, 1984). The variability in the levels was large. At the individual level, the data showed both increase and decrease in blood levels relative to pre-exposure levels, which was attributed by the authors as plausibly due to temporal variations in baseline levels in humans, particularly since the experiment did not control food intake prior to exposure. Studies in rhesus monkeys have revealed endogenous formaldehyde levels (2.4 μg/g blood) comparable to humans and that levels were also unaltered following exposure to 6 ppm formaldehyde via inhalation 6 hours/day for 4 weeks, measurements being taken at both 7 minutes and 45 hours post final exposure (Casanova et al., 1988).

It is important to keep in mind that the GC-MS method is not capable of detecting irreversibly bound formaldehyde; for example, formaldehyde levels detected by this method, even in the anterior nasal mucosa of rats exposed to 6 ppm of formaldehyde, were not elevated over control levels. Furthermore, the GC-MS method does not differentiate between free and reversibly bound adducts of formaldehyde (Heck et al., 1982). Thus, measured levels represent total formaldehyde concentration that includes free formaldehyde as well as reversibly bound adducts. Based on the known Michaelis-Menten constant, Km, for formaldehyde dehydrogenase with respect to the GSH adduct formation, Heck et al. (1982) estimated under certain assumptions that free formaldehyde comprised only about 1–2% of the total formaldehyde measured by their method. Furthermore, as shown by Metz et al. (2006, 2004), formaldehyde reactions with primary amino and thiol groups can, in a second step, react with many other amino acids to form stable methylene bridges. Presumably, such reactions would not be detectable by using the methods employed by Heck et al. (1982).[4] Thus, the limited interpretation of GC-MS measurements of blood levels suggests that formaldehyde does not appreciably reach the blood, is rapidly metabolized or interacts with macromolecules when it escapes metabolism, or is otherwise undetected.

Results from an earlier experiment using radiolabeled formaldehyde in rats are consistent with the conclusion based on the GC-MS measurements of no appreciable increase in blood levels of formaldehyde. Following a 6-hour exposure of F344 rats to 15 ppm of [^{14}C]-formaldehyde (Heck et al., 1983), the concentrations of ^{14}C in the nasal mucosa were 28-fold higher than those in the blood. The observed half-life of the terminal phase of the radioactivity was long (55 hours); on the other hand, it is known that the half-life of free formaldehyde in the rat blood is very short. Therefore, the authors concluded that the radioactivity was likely due to modification of macromolecules or metabolic incorporation rather than slow metabolic clearance of formaldehyde. The terminal decline of the radioactivity in the packed cell fraction of the blood was much slower and observed to be consistent with incorporation into erythrocytes.

In the same paper, Heck et al. (1983) report on the similarity in the pharmacokinetics of radiolabeled formaldehyde and radiolabeled formate in the rat blood, supporting their hypothesis that oxidation of formaldehyde to formate and subsequent incorporation of this compound through one-carbon metabolism were major factors in the disposition of formaldehyde. Studies by Gottschling et al. (1984) have also established that the main product of metabolic clearance of

---

[4] Additionally, note that, although Heck et al. (1982) demonstrated that formaldehyde concentration can be accurately measured from glutathione and tetrahydrofolate adducts, similar experiments were not performed by using protein samples or cellular extracts (i.e., in the presence of various amino acids). In addition, standard curves for predicting formaldehyde concentration in tissues were generated in aqueous solutions rather than biological samples.

formaldehyde is formate, which is either further metabolized to CO_2 and water, incorporated into the one-carbon pool, and/or eliminated in the urine as a sodium salt at about 13 mg/L urine.

3.3.2. Levels in Various Tissues

The radiolabeling studies indicated high levels of ^{14}C in the rat nasal mucosa (equivalent concentrations of ^{14}C-formaldehyde in the nasal mucosa of rats naïvely exposed to 15 ppm ^{14}C-formaldehyde were 2,148 ± 255 nmol/g compared with 76 ± 11 nmol/g in plasma). In contrast, the GC-MS studies did not detect elevated formaldehyde in this region. This is not to be interpreted as a discrepancy, because the radiolabeling study did not distinguish among radiolabeled species and thus the measured radioactivity could potentially be free or bound formaldehyde, formate, or any [^{14}C] metabolically incorporated into macromolecules.

In concurrent studies, Casanova-Schmitz et al. (1984) resolved the question as to whether the higher [^{14}C] levels in the nasal mucosa were a consequence of GSH depletion and a subsequent reduction in GSH-dependent clearance of formaldehyde. An important result in these studies was that there was no significant difference in labeling in either the nasal mucosa or in plasma between naïve F344 rats and those pre-exposed to unlabeled 15 ppm formaldehyde 6 hours/day for the 9 previous days. These findings indicated little or no apparent effect on the disposition of formaldehyde following short-term exposure to relatively high levels of formaldehyde. In contrast, Farooqui et al. (1986) reported decreases in GSH in several tissues 3 hours after a sublethal I.P. injection of formaldehyde but not after 6 and 9 hours. Taken together, these data suggest that formaldehyde exposure does not result in long-term alterations in cellular GSH levels and that repeated inhalation exposure does not alter the dosimetry to the bloodstream or formaldehyde body burden.

Heck et al. (1983) determined the ^{14}C concentrations in different tissues in the F344 rat body by exposing rats in a head-only chamber to various concentrations (5–24 ppm) of radiolabeled formaldehyde for 6 hours. (Concentrations of ^{14}C in internal organs and tissues relative to that in plasma did not appear to vary much as exposure concentrations increased; therefore only averages over the concentration range were reported.) Except for the esophagus, levels in the heart, spleen, lung, intestines, liver, and kidney were 1–3 times higher relative to that in plasma. Labeling in the esophagus was high (fivefold relative to plasma). The authors attributed this relatively higher dose to mucociliary action in the nose and trachea. The data also indicate that the brain, testes, and erythrocytes appear to have about threefold lower ^{14}C levels than plasma. Pre-exposure to formaldehyde (for 9 days) did not alter the measured radioactivity in the nasal mucosa or plasma. Thus, it was concluded that the single exposure findings may also be qualitatively extended to chronic exposures.

The total radiolabel measured in the bone marrow (femur) of F344-rats exposed for 6 hours to 0.3–15 ppm of radiolabeled formaldehyde in the Casanova et al. (1984) experiment was high (generally within a factor of 0.5 of the total labeling in the nasal respiratory mucosa). Nearly half of the ^{14}C was contained in the DNA in this tissue presumably on account of the high rate of cell turnover in the bone marrow, indicating that the carbon derived from ^{14}C-formaldehyde was utilized for DNA synthesis (Casanova-Schmitz et al., 1984).

Chang et al. (1983) described visceral labeling (via autoradiography) in rats, following exposure to 15 ppm [^{14}C]-formaldehyde 6 hours/day for 4 days. The authors attributed this labeling to mucociliary clearance and grooming-related ingestion of formaldehyde.

In summary, following exposure to radiolabeled formaldehyde, the radioactivity was very high in the nasal mucosa but was also extensively distributed to various tissues. In particular, levels in the bone marrow were high. On the other hand, formaldehyde levels in the blood measured by GC-MS were not significantly elevated. Thus, the authors considered it unlikely that the elevated ^{14}C in various tissues was due to free formaldehyde. Instead, these levels were thought to arise from either rapid metabolic incorporation or formation of covalent adducts or incorporation via carboxylation reactions of the $^{14}CO_2$ formed during metabolism.

The data presented thus far in this section illustrate that measuring the distribution of the absorbed formaldehyde based on ^{14}C-radiolabeling and GC-MS studies alone is problematic because it is difficult to resolve (through these studies) whether it is free, reversibly bound, irreversibly bound, formate, one-carbon pool, etc. This is of significance with regard to understanding the availability of the absorbed formaldehyde. More indirect methods had to be developed to further examine the disposition of formaldehyde; however, as discussed below, the interpretation of these approaches may also not be straightforward.

3.3.2.1. *Disposition of Formaldehyde: Differentiating Covalent Binding and Metabolic Incorporation*

The motivation in presenting this section is twofold, as follows:

1. As concluded above, subsequent studies were necessary to ascertain whether measured radiolabeling in different experiments was due to formaldehyde adducts or incorporation of [^{14}C] one-carbon units of formaldehyde into macromolecules via the one-carbon pool.
2. DNA protein cross-links (DPXs) formed by formaldehyde (covalently bound in this case) have been regarded as a surrogate dose metric for the intracellular concentration of formaldehyde (Hernandez et al., 1994; Casanova et al., 1991, 1989). This is particularly relevant because of the nonlinear dose response for DPX formation due to saturation of

enzymatic defenses at high concentrations (Casanova et al., 1991, 1989). Thus, the ability to measure DPX is an important development.

An important question is whether the formaldehyde disposed in the form of DPX is detected in remote tissues. A set of elegant but complex experiments involving dual isotope labeling (^{14}C and ^{3}H) was carried out to this end by the Heck and Casanova-Schmitz and their coworkers. Casanova-Schmitz et al. (1984) and Casanova-Schmitz and Heck (1983) used dual isotope labeling of formaldehyde as a way to partially distinguish between formaldehyde adducts formation and metabolic incorporation. In separate experiments, F344 rats were exposed to ^{3}H- and ^{14}C- formaldehyde at different exposure concentrations (0.3–15.0 ppm), and the $^{3}H/^{14}C$ ratios of different phases of DNA were measured. Only the highlights of the results and significant issues are presented here. The overall conclusions from these experiments were as follows:

- Labeling in the nasal mucosa was due to both covalent binding and metabolic incorporation.
- DPX was formed at 2 ppm and greater concentrations in the respiratory mucosa.
- In the bone marrow, formaldehyde did not bind covalently to bone marrow macromolecules at any exposure concentration. The labeling of bone marrow macromolecules was found to be entirely due to metabolic incorporation and not due to covalent binding.

Macromolecules such as DNA and protein can be isolated from tissue homogenates by extraction into three phases: an organic phase consisting of proteins, an aqueous phase consisting of only double-stranded DNA, and an interfacial phase consisting of both DNA and protein. Single-stranded (but not double-stranded) DNA was particularly likely to form adducts. DNA from this interfacial phase can be further purified and has been shown to consist of DPXs (Casanova-Schmitz and Heck, 1983). Because both [^{14}C]-formaldehyde and [^{3}H]-formaldehyde can become incorporated into DNA and protein metabolically as well as by cross-linking, the $^{3}H/^{14}C$ ratio in such cross-linked material should be higher than in material that primarily contains metabolically incorporated formaldehyde. Figure 3-2 shows the labeling of tissue from the nasal respiratory mucosa and bone marrow (distal femur) in rats exposed to [^{14}C]-formaldehyde and [^{3}H]-formaldehyde vapor.

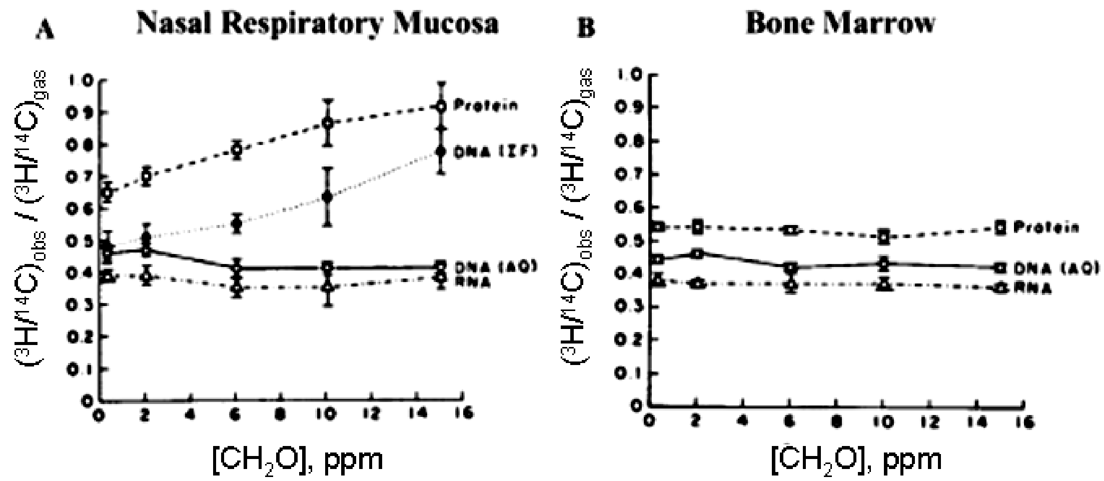

Figure 3-2. $^3H/^{14}C$ ratios in macromolecular extracts from rat tissues following exposure to ^{14}C- and ^3H-labeled formaldehyde (0.3, 2, 6, 10, 15 ppm).

Note that the small yield of interfacial (IF) phase from bone marrow tissue precluded further analysis; this is *prima facie* evidence for the lack of significant DPXs in this tissue.

Source: Casanova-Schmitz et al. (1984a).

In the nasal mucosa the interfacial phase has a significantly higher $^3H/^{14}C$ ratio than the material in the aqueous phase. This suggests that interfacial DNA has significantly more ^3H, a phenomenon likely explained by additional [^3H]-formaldehyde molecules present as DPXs prior to extraction. The amount of interfacial DNA was found to have a clear dose response. These cross-links were also judged to be due to exogenous formaldehyde. Likewise, the organic phase of the nasal mucosa showed a similar increase in $^3H/^{14}C$ ratio at higher concentrations, a result that could be attributed to various inter- and intra-protein adducts (Metz et al., 2004; Trezl et al., 2003; Skrzydlewska, 1996).

In contrast, analysis of macromolecules at the distal femur location presents a different pattern (Figure 3-2, part B). First, the interfacial phase was not detected during extraction, suggesting that there were few or no DPXs to be detected. Second, there was no increase in $^3H/^{14}C$ ratio in the organic (i.e., protein) phase as a function of dose. Therefore, it was concluded that either radiolabeled formaldehyde or formate reached the distal site and was subsequently incorporated into macromolecules. According to the mechanistic interpretation of these studies, the quantity plotted on the ordinate in Figure 3-2 (the ratio of $^3H/^{14}C$ between the tissue and the exposure gas) should approach unity as metabolism becomes saturated and more adduct formation occurs, particularly for protein. Indeed, this is what is observed (see Figure 3-2, part A). In contrast, there is no dose effect in the femur, suggesting that the labeling at all doses in that tissue may be due to metabolic incorporation and not due to the parent formaldehyde.

(Note: These data were originally shown in the absence of an analysis of isotope effects on covalent binding and metabolism. Subsequent studies determined that [^{3}H]-formaldehyde is oxidized less rapidly than [^{14}C]-formaldehyde and unlabeled formaldehyde. This suggests that the ^{3}H/^{14}C ratio, and therefore the amount of formaldehyde covalently bound to tissue, is likely overestimated because more [^{3}H]-formaldehyde remains unmetabolized, i.e., free to bind [Heck and Casanova, 1987]. The authors hypothesized that this overestimate was relatively greater at the lower concentrations.)

Similar results were obtained in GSH-depleted rats (Casanova and Heck, 1987). Again, these authors observed a dose-dependent increase in the ^{3}H/^{14}C ratio in the interfacial DNA and organic fractions of disrupted cells of the respiratory and olfactory mucosa and no such increases in bone marrow. Interestingly, at 10 ppm exposure (only), GSH-depleted rats exhibited a higher ^{3}H/^{14}C ratio in the organic phase than did normal rats. Casanova and Heck (1987) posited that much of the covalent binding at 6 ppm and lower was due to binding to extracellular proteins, whereas the higher ^{3}H/^{14}C ratio in GSH-depleted rats at 10 ppm was due to more intracellular binding.

In their first experiment to measure DPX concentrations, Casanova-Schmidt et al. (1984) and Casanova and Heck (1987) used the dual isotope method (^{3}H/^{14}C) mentioned above. In this experiment, DPX was observed only at formaldehyde concentrations ≥2 ppm. Subsequently, Casanova et al. (1989) developed a more sensitive method using high-performance liquid chromatography (HPLC) for measuring DPX. In this method, tissue homogenates were digested with a proteolytic enzyme and extracted with a phenolic solvent. DPX was detected in the nasal mucosa of rats at formaldehyde concentrations as low as 0.3 ppm. This method was also used to measure DPX in the nasal region, the larynx, trachea and carina, and major intrapulmonary airways (airway diameters > 2mm) of rhesus monkeys exposed for 6 hours to 0.7, 2.0 and 6.0 ppm of formaldehyde. DPX was detected in the nose (including the nasopharynx) at all concentrations and at 2.0 and 6.0 ppm in the larynx, trachea, carina and other lower airways. However, DPX was not detectable in the bone marrow of these monkeys at any concentration.

Overall, Heck and Casanova-Schmitz and their coworkers interpreted the results of these various experiments to mean that inhaled formaldehyde could not reach distant sites in the body. It may be noted in this context that Shaham et al. [1996] reported elevated DPX levels in the white blood cells of laboratory workers exposed to formaldehyde. These data are further reported in Chapter 4.)

3.4. METABOLISM

Formaldehyde is primarily metabolized by glutathione-dependent formaldehyde dehydrogenase (FALDH) and aldehyde dehydrogenases (ALDHs). Numerous studies now recognize FALDH as a member of the alcohol dehydrogenase (ADH) family, specifically ADH3 (Thompson et al., 2009; Liu et al., 2004, 2001; Hedberg et al., 2003; Høøg et al., 2003; and the references in each of these). The remainder of this report will refer to FALDH as ADH3.

3.4.1. In Vitro and In Vivo Characterization of Formaldehyde Metabolism

Formaldehyde is oxidized to formate by two metabolic pathways (Figure 3-3). The first pathway involves conversion of free formaldehyde to formate by the so-called low-K_m (K_m = 400 µM) mitochondrial aldehyde dehydrogenase-2 (ALDH2). The second pathway involves a two-enzyme system that converts glutathione-conjugated formaldehyde (S-hydroxymethylglutathione [HMGSH]) to the intermediate S-formylglutathione, which is subsequently metabolized to formate and GSH by S-formylglutathione hydrolase.

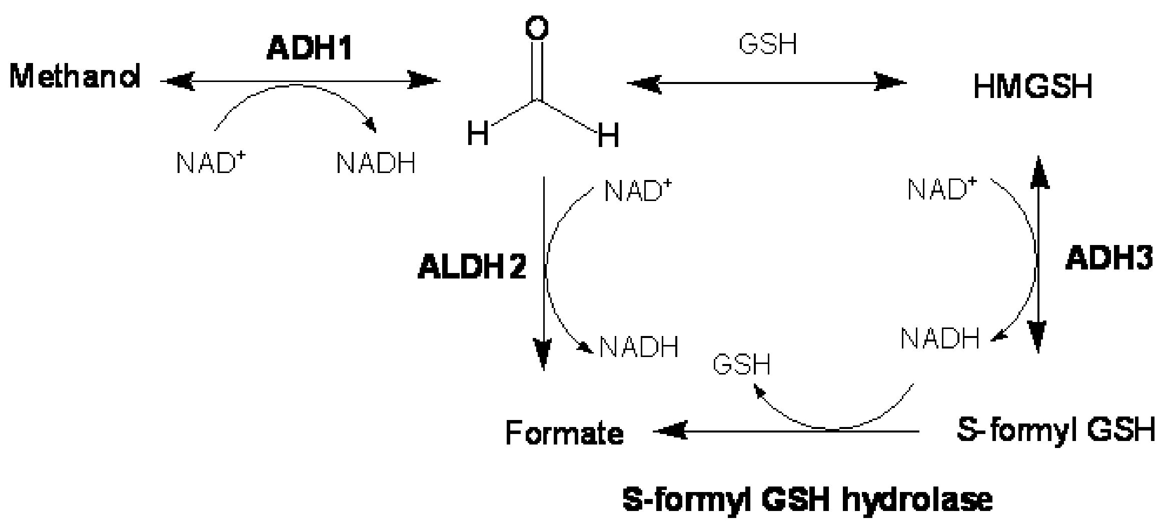

Figure 3-3. Formaldehyde clearance by ALDH2 (GSH-independent) and ADH3 (GSH-dependent).

The K_m value for ALDH2 and free formaldehyde is about 400 µM (Teng et al., 2001), whereas the K_m value for HMGSH and ADH3 is 6.5 µM (Uotila and Koivusalo, 1974a,b). The ADH-mediated reactions are reversible in the presence of excess reduced nicotinamide adenine dinucleotide (NADH).
Source: Adapted from Teng et al. (2001).

Though ADH3 is rate limiting in this second pathway, the affinity of HMGSH for ADH3 (K_m = 6.5 µM) is about 100-fold higher than that of free formaldehyde for ALDH2. In addition to the kinetic properties, this member of the ADH gene family (Høøg et al., 2003, 2001; Liu et al., 2001; Jornvall et al., 2000; Estonius et al., 1996) appears to be ubiquitously expressed in organ tissues (Molotkov et al., 2002; Ang et al., 1996a, b), exhibits cytoplasmic and nuclear localization (Fernandez et al., 2003), and is the most abundant ADH family member in the liver and brain (Galter et al., 2003).

In vitro studies have examined the clearance of formaldehyde in several human and rat tissues (Table 3-2). Examination of formaldehyde metabolism in the rat nasal and olfactory mucosa indicates nearly identical pharmacokinetics in the rat liver on a per mg of cell lysate basis (Casanova-Schmitz et al., 1984b). Similar results have been obtained in the absence of GSH, where other ALDH family members oxidize formaldehyde, albeit with significantly lower affinity (i.e., higher K_m). Hedberg et al. (2000) demonstrated that human buccal tissue lysate kinetics are in close agreement with those reported for purified human liver ADH3 (Uotila and Koivusalo, 1974a). Additionally, micro-array analysis indicates that these cells express far more ADH3 and S-formylglutathione hydrolase than ALDH1 or ALDH2 (Hedberg et al., 2001a). The results of Ovrebo et al. (2002) are not easily compared with the other studies in Table 3-2 because these studies were in intact cell cultures. However, it is apparent that the pharmacokinetic values in these human cells are comparable to intact rat liver cells.

Table 3-2. Formaldehyde kinetics in human and rat tissue samples

Source	K_m (µM)	V_{max} (nmol/mg protein × min)	Reference
Purified human liver ADH3	6.5	2.77 ± 0.12	Uotila and Koivusalo (1974a, b)
Rat olfactory mucosa (+ GSH)	2.6 ± 0.5	1.77 ± 0.12	Casanova-Schmitz et al. (1984b)
Rat olfactory mucosa (− GSH)	647 ± 43	4.39 ± 0.14	Casanova-Schmitz et al. (1984b)
Rat respiratory mucosa (+ GSH)	2.6 ± 2.6	0.90 ± 0.24	Casanova-Schmitz et al. (1984b)
Rat respiratory mucosa (− GSH)	481 ± 88	4.07 ± 0.35	Casanova-Schmitz et al. (1984b)
Rat liver (+ GSH)	5.0 ± 1.9	2.0 ± 0.3	Casanova-Schmitz et al. (1984b)
Human bronchial explants[a]	5,100	3.3	Ovrebo et al. (2002)
Human bronchial epithelial[a]	1,400	6.1	Ovrebo et al. (2002)
Rat hepatocytes[a]	1,250	4.2	Ovrebo et al. (2002)
Human buccal tissue (+ GSH)	11 ± 2	2.9 ± 0.6	Hedberg et al. (2000)
Human buccal tissue (− GSH)	360 ± 90	1.2 ± 0.7	Hedberg et al. (2000)
Human keratinocytes	n.d.[b]	14.5 ± 1.8	Hedberg et al. (2000)
Human fibroblasts	n.d.	17.9 ± 1.4	Hedberg et al. (2000)

[a]These studies were carried out in intact cells by measuring the formation of formate. This likely explains the nearly 1,000-fold increase in apparent K_m, since much of the formaldehyde was likely to be bound extracellularly. The remaining studies used either purified enzyme or cell lysates (as indicated) and measured the formation of NADH.
[b]n.d. = not determined.

The data in Table 3-3 along with data indicating the ubiquity of ADH3, indicate that many human tissues and cells, particularly in the respiratory tract, appear to exhibit significant capacity to metabolize formaldehyde. Molecular biology techniques have demonstrated the importance of ADH3 in formaldehyde clearance. For example, ADH-knockout studies have shown that the median lethal dose (LD_{50}) values for formaldehyde in wild type, $ADH1^{-/-}$, $ADH3^{-/-}$, and $ADH4^{-/-}$ mice strains were 0.200, 0.175, 0.135, and 0.190 g/kg, respectively (Deltour et al., 1999). Although the statistical significance was not reported, the data indicate that deletion of ADH3 increases the sensitivity of mice to formaldehyde.

The pharmacokinetics of formate are complex. Formate can undergo adenosine triphosphate (ATP)-dependent addition to tetrahydrofolate (THF), which can carry either one or two one-carbon groups. Formate can conjugate with THF to form N^{10}-formyl-THF and its isomer N^5-formyl-THF, both of which can be converted to N^5,N^{10}-methenyl-THF and subsequently to other derivatives that are ultimately incorporated into DNA and proteins via biosynthetic pathways (Figure 3-4).

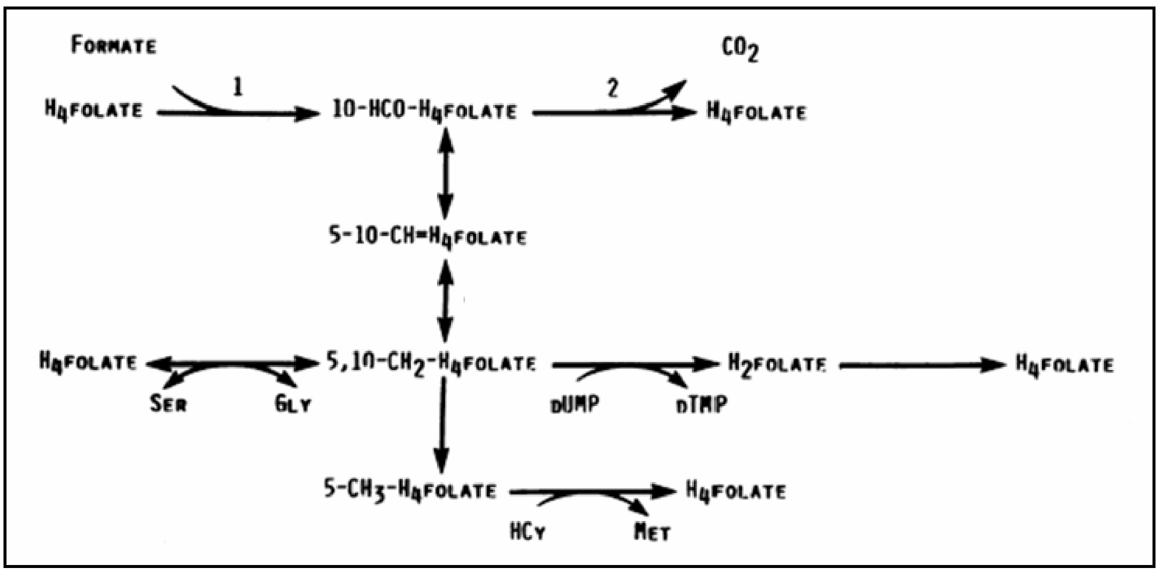

Figure 3-4. Metabolism of formate.
Note: 1, formyl-THF synthetase; 2, formyl-THF dehydrogenase.

Source: Adapted from Black et al. (1985).

Elevated levels of formate in urine have been detected following inhalation of methanol or formate under certain conditions (Liesivuori and Savolainen, 1987), although the interpretation of this finding is unclear. There is also evidence that formate generates CO_2^-

radicals and can be metabolized to CO_2 via catalase and via the oxidation of N^{10}-formyl-THF (Dikalova et al., 2001, and references therein). The significance of formate in formaldehyde toxicity is unclear. Black et al. (1985) reported that hepatic tetrahydrofolate levels in monkeys are 60% of those in rats and that primates are far less efficient in clearing formate than are rats and dogs. Studies involving [^{14}C]-formate suggest that about 80% is exhaled as $^{14}CO_2$, 2–7% is excreted in the urine, and about 10% undergoes metabolic incorporation (Hanzlik et al., 2005, and references therein). Mice deficient in formyl-THF dehydrogenase exhibit no change in LD_{50} (via I.P. dose) for methanol or in oxidation of high doses of formate (Cook et al., 2001). It has been suggested that rodents efficiently clear formate via folate-dependent pathways, peroxidation by catalase, or an unknown third pathway. Conversely, primates do not appear to exhibit such capacity and are more sensitive to metabolic acidosis following methanol poisoning (Cook et al., 2001).

3.4.2. Formaldehyde Exposure and Perturbation of Metabolic Pathways

The enzyme ADH3 has received renewed attention in recent years because of new functions that have been attributed to it. ADH3 is central to the metabolism of formaldehyde; however, exposure to formaldehyde in turn alters the activity of ADH3 (in multiple dose-dependent ways), thereby leading to perturbation of critical metabolic pathways. These are briefly mentioned below (refer to cited papers for details).

1. Exposure to formaldehyde increases cell replication. These proliferating epithelial and inflammatory cells are rich in both the messenger ribonucleic acid (mRNA) and protein of ADH3 (Nilsson et al., 2004; Hedberg et al., 2000). Studies in the rodent lung suggest that increases in ADH3 in such cells dramatically alter the biology of other important ADH3 substrates that are involved in protein modification and cell signaling (Que et al., 2005).
2. ADH3 also participates in the oxidation of retinol and long-chain primary alcohols, as well as the reduction of S-nitrosoglutathione (GSNO) (Staab et al., 2009; Thompson et al., 2009; Hedberg et al., 2003; Høøg et al., 2003; Molotkov et al., 2002; Liu et al., 2001; Jornvall et al., 2000; Jensen et al., 1998). The activity of ADH3 toward some of these substrates has been shown to be significantly increased in the presence of formaldehyde. Staab et al. (2009) showed that (in cultured cells) GSNO can accelerate ADH3-mediated formaldehyde oxidation and, likewise, that formaldehyde increases ADH3-mediated GSNO reduction nearly 25-fold. The following effects may be noted with regard to the relevance of such perturbations.

a. GSNO is an endogenous bronchodilator and reservoir of nitric oxide (NO) activity (Jensen et al., 1998). Details on the ADH3-mediated reduction of GSNO are shown in Thompson and Grafstrom (2008).
b. ADH3 is implicated in playing a central role in regulating bronchiole tone and allergen-induced hyperresponsiveness (Gerard, 2005; Que et al., 2005).
c. As concluded by California Environmental Protection Agency (CalEPA) (2008), "the dysregulation of NO by formaldehyde [in this manner] helps to explain the variety and variability in the toxic manifestations following formaldehyde inhalation."

3.4.3. Evidence for Susceptibility in Formaldehyde Metabolism

Teng et al. (2001) provided evidence that inhibition of ADH1, ALDH2, and ADH3 has significant impact on formaldehyde toxicity. The authors speculated that deficiencies in any of these enzymes would confer an increased susceptibility to formaldehyde toxicity (Teng et al., 2001). Polymorphism in ALDH2 has been shown to have implications in human risk assessment, specifically with regard to acetaldehyde metabolism (Ginsberg et al., 2002). It is worth noting, however, that Teng et al. (2001) only demonstrated the importance of ALDH2 in rat hepatocytes with formaldehyde concentrations of 2.5 mM and greater. Since this concentration is fivefold greater than the 0.5 mM K_m for free formaldehyde, ALDH2 involvement is not unexpected at such high concentrations. Teng et al. (2001) also demonstrated the importance of ADH1 in driving the reverse reaction (i.e., formaldehyde to methanol) by coadministration of NADH-generators. This would have the effect of prolonging the life of formaldehyde by continuous recycling. This is not surprising, given that many ADH reactions are reversible. However, levels of nicotinamide adenine dinucleotide (NAD^+) are normally much higher than NADH.

To date, two studies have reported polymorphisms in ADH3, using the new nomenclature.[5] ADH3 transcription appears to be regulated by specificity protein (Sp1), with a minimal promoter located at positions −34 to +61. The reported polymorphisms in ADH3 involve four base-pair substitutions in the promoter region and no polymorphisms in the coding region (Hedberg et al., 2001b). The three polymorphisms include −197/−196 (GG→AA), −79 (G→A), and +9 (C→T). The genotype frequencies are shown in Table 3-3. Of these alleles, the +9 (C→T) polymorphism (in the putative Sp1 minimal promoter region) reduced transcriptional

[5] Other epidemiologic studies investigating links between ADH3 and oral cancer use the older nomenclature and thus refer to Class I ADH (i.e., ADH1) enzymes.

activity twofold in in vitro reporter gene experiments. According to Hedberg et al. (2001b), no studies have demonstrated differences in ADH3 enzyme activity in humans. More recently, single nucleotide polymorphisms in ADH3 have been reported to be associated with childhood risk of asthma, although the functional relevance of these polymorphisms has not been published (Wu et al., 2007).

Table 3-3. Allelic frequencies of ADH3 in human populations

Allele frequencies (%)									
Population, n		**AA$_{-197/-196}$**	**GG$_{-197/-196}$**		**A$_{-79}$**	**G$_{-79}$**		**T$_{+9}$**	**C$_{+9}$**
Chinese, 83		22	78		100	–		–	100
Spanish, 95		41	59		62	38		–	100
Swedish, 96		47	53		67	33		1.5	98.5

Source: Adapted from Hedberg et al. (2001b).

Alterations in THF pathways may also have an impact on formaldehyde toxicity. These could result from polymorphisms in various enzymes or differences in folate intake and absorption. Species differences in tetrahydrofolate levels (Black et al., 1985) are thought to play a role in the differential responses to methanol across species. Cook et al. (2001) speculate that rats have redundant pathways for formate clearance that may be absent or less efficient in primates.

3.5. EXCRETION

The main product of metabolic clearance of formaldehyde is formate, which is further metabolized to CO_2 and water, incorporated into the one-carbon pool, or eliminated in the urine. There is also some evidence that formaldehyde is present in exhaled breath; however, it is unclear whether this originates from endogenous sources, or is simply a function of ambient formaldehyde dissolved in fluids lining POEs. The following sections describe first experiments in laboratory species and then available data in humans. Broadly, these studies address two important questions that may be of relevance for risk assessment. First, it may be of interest to know what levels of formaldehyde are exhaled for comparison with inhaled levels, and whether there is any relationship between external exposure and exhaled levels. Second, there are recent studies that have attempted to relate genetic polymorphisms and changes in gene transcription level to levels of putative urinary formaldehyde biomarkers.

3.5.1. Formaldehyde Excretion in Rodents

Heck et al. (1983) determined the relative contributions of various excretion pathways in F344 rats following inhalation exposure to formaldehyde. Table 3-4 indicates that the relative excretion pathways were independent of exposure concentration (at least between 0.63 and 15 ppm). Nearly 40% of inhaled [^{14}C]-formaldehyde appeared to be eliminated via expiration, probably as CO_2 (it should be recalled that nearly 100% of inhaled formaldehyde is absorbed). Within 70 hours of a 6-hour exposure to formaldehyde, about 17 and 5% were eliminated in the urine and feces, respectively. Nearly 40% of inhaled [^{14}C]-formaldehyde remained in the carcass, presumably due to metabolic incorporation.

Table 3-4. Percent distribution of airborne [^{14}C]-formaldehyde in F344 rats

Source	Concentration of formaldehyde (ppm)	
	0.63	13.1
	Distribution (%)[a]	
Expired air	39.4 ± 1.5	41.9 ± 0.8
Urine	17.6 ± 1.2	17.3 ± 0.6
Feces	4.2 ± 1.5	5.3 ± 1.3
Tissues and carcass	38.9 ± 1.2	35.2 ± 0.5

[a]Values are means ± standard deviations (n = 4).

Source: Heck et al. (1983).

Mashford and Jones (1982) examined elimination pathways of formaldehyde in rats exposed by I.P. injection. Urine and exhaled gases were collected from rats exposed to 4 or 40 mg/kg [^{14}C]-formaldehyde. At 48 hours postinjection, 82 and 78% of the radiolabel were exhaled as $^{14}CO_2$, whereas exhaled [^{14}C]-formaldehyde was not detected. Mashford and Jones (1982) also further identified the urinary metabolites. Five hours after injection of the higher dose, formate was determined to comprise 80% of the urinary metabolites. The authors were unable to detect cysteine derivatives observed in other studies (see below) in the urine of these rats prior to or after formaldehyde exposure. The authors stated that if formaldehyde were to be excreted in urine containing cysteine, then thiazolidine-4-carboxylate (TZCA) would likely be produced. They speculated that species differences in urinary compounds may produce formaldehyde conjugates (or artifacts).

Hemminki (1982) reacted formaldehyde and acetaldehyde with cysteine, N-acetylcysteine, and GSH and found that formaldehyde reacted most rapidly with cysteine to form TZCA. Similarly, acetaldehyde reacted preferentially with cysteine, albeit slower than formaldehyde, to form a thiazolidine derivative. However, when each aldehyde was administered I.P. (10% formaldehyde, 50% acetaldehyde), thioether concentrations (nmol/mol creatinine) significantly increased in the 24 and 48 hour urine of acetaldehyde-treated rats but not formaldehyde-treated rats. These data suggest that formaldehyde is not appreciably excreted in urine and thus cysteine conjugates are not likely to represent formaldehyde exposure.

Most recently, Shin et al. (2007) attempted to show that formaldehyde inhalation increased urinary TZCA levels in Sprague-Dawley rats. Treated rats were exposed to 3.1 and 38.1 ppm formaldehyde for 6 hours/day for 2 weeks, and urine was collected for 3 days. The TZCA level in four control rats was 0.07 ± 0.02 mg/L, whereas levels in the 3 and 38 ppm groups were 0.18 ± 0.045 and 1.01 ± 0.36, respectively. Notably, the concentrations in the four highest exposed animals (0.71, 0.70, 1.20, and 1.43 ppm) exhibited a nearly twofold range. However, these comparisons are confounded if the exposures have any influence on urine production and urine cysteine levels. The study does not provide any data that might allow one to examine this issue.

3.5.2. Formaldehyde Excretion in Exhaled Human Breath

Several human and animal studies have attempted to measure the concentration of formaldehyde in exhaled breath. None of the human studies were designed to distinguish between exogenous (room air) and endogenous (systemic) formaldehyde in exhaled breath. In order to discern whether endogenous formaldehyde is excreted into the lungs, test subjects must breathe formaldehyde-free air. Because subjects were breathing room air, which contained 9-10 ppb formaldehyde in two studies and unspecified concentrations in two other studies, it is impossible to ascertain whether there was any endogenous formaldehyde in their exhaled breath. One study demonstrates that the formaldehyde concentration is lower in exhaled breath than in inhaled breath (Cáp et al., 2008). Also, none of the human studies investigated whether there is any relationship between exhaled formaldehyde levels and food intake, life stage, smoking, or health status. This assessment identifies a critical research need for further studies on the measurement of exhaled formaldehyde.

Proton transfer reaction mass spectrometry (PTR-MS) has been applied to measure trace compounds in exhaled breath including volatile organics and specifically formaldehyde. The basic method of PTR-MS is based on the transfer of protons from H_30^+ to gases in exhaled breath and the in-line monitoring of products where gases are tentatively identified by the mass to charge ratio (*m/z*) where a *m/z* of 31 is consistent with protonated formaldehyde (Hansel et al., 1995; Lindinger et al., 1998). It is important to note that reaction products from methanol and ethanol may also produce fragments with an *m/z* ratio of 31 (Kusch et al., 2008). Up to 1% of the mass of ethanol and methanol in exhaled breath may be detected with an *m/z* ratio of 31 and thus be identified as formaldehyde, so accurate quantitation of formaldehyde should adjust for this contribution (Španěl and Smith, 2008). Selected ion flow tube mass spectrometry (SIFT-MS) is an application of PTR-MS developed for real-time analysis of trace gases in breath (Smith and Španěl, 2005; Španěl and Smith, 2007).

Moser et al. (2005) measured levels of 179 volatile organic compounds (VOCs) in the exhaled breath of 344 individuals. This study was not designed to ascertain whether exhaled formaldehyde is of endogenous origin, but rather to demonstrate that proton transfer reaction-mass spectrometry can be used as a new method for rapid screening of large collectives for risk factors (e.g., smoking behavior), potential disease biomarkers, and ambient air characterization. The study was conducted at a health fair. The test subjects had a mean age of 61.6 years; 63% were males and 14% were smokers. Samples of room air were collected and evaluated in parallel with exhaled breath samples. The authors note that formaldehyde was detected in room air, but did not report the levels; rather they stated that the background concentrations were negligible. Of the 179 volatile organic compounds measured, data were reported for 14, including formaldehyde and formic acid. The formaldehyde levels in exhaled breath spanned from 1.2 to 72.7 ppb with a median of 4.3 ppb and 75th percentile of 6.3 ppb. No explanation was provided for this wide range in values, and there was no distinction of the data by sex, age, health, or smoking status.

Because the test subjects were breathing ambient indoor air which contained an unspecified concentration of formaldehyde, it is impossible to ascertain whether exhaled formaldehyde was from an endogenous or exogenous source, or both. Moser et al. also note that significant differences in exhaled breath composition could be found between smokers and non-smokers for 32 of the 179 chemicals measured, but the 32 chemicals were not named and no substantiating data were provided. Formaldehyde may have been among these 32 chemicals since it is a major component of cigarette smoke (NLM, 2001).

The report by Moser et al. does not provide the limit of detection for any of the compounds measured or details of the analytical method. The minimum formaldehyde level reported in exhaled breath was 1.23 ppb. The method employed by Moser et al. does not adjust the detection of apparent formaldehyde (*m/z*) by accounting for the contribution of methanol and ethanol. The levels of methanol and ethanol in exhaled breath were reported, however. Based on 1% of the mass of these chemicals contributing to the $m/z = 31$ in the PTR-MS method (Španěl and Smith, 2008), Table 3-5 demonstrates that the highest formaldehyde levels reported may have been an artifact of high methanol and ethanol in exhaled breath. Because the in-room formaldehyde concentrations were not reported, it is unknown how much of this formaldehyde represents formaldehyde levels in inhaled air. Additionally, since these samples were simple exhaled breath samples and not SIFT-MS samples, it is impossible to distinguish between air which reached the pulmonary region versus air which only entered the upper airways.

Table 3-5. Apparent formaldehyde levels in exhaled breath of individuals attending a health fair, adjusted for methanol and ethanol levels which contribute to the detection of the protonated species with a mass to charge ratio of 31 reported as formaldehyde (*m/z* = 31)

Chemical	Minimum	25^{th} percentile	Median	75^{th} percentile	97.5^{th} percentile	Maximum
Methanol (*m/z* = 31)	13.367	106.227	161.179	243.185	643.614	1536.499
1% of methanol predicted as *m/z* = 31	0.13	1.06	1.61	2.43	6.44	15.36
Ethanol	11.583	23.1	34.664	64.24	549.24	9779.768
1% of ethanol predicted as *m/z* = 31	0.12	0.23	0.35	0.64	5.49	97.80
Mass of *m/z* = 31 attributable to methanol and ethanol	0.25	1.29	1.96	3.07	11.93	113.16
Mass of *m/z* = 31 reported as formaldehyde	1.23	3.1	4.26	6.33	39.8	72.7

Source: Moser et al. (2005).

Turner et al. (2008) compared levels of volatile compounds in exhaled breath to levels in emissions from the skin in five males (3 in their mid 20s, and the others 42 and 49 years old). The subjects fasted overnight, and measurements were taken before and after ingesting 75 g of glucose. The source of the inhaled air was laboratory air which contained an unreported concentration of formaldehyde. Formaldehyde was not detected in the exhaled breath of any subjects. The limit of detection was 5 ppb or better.

Wang et al. (2008) measured the concentrations of formaldehyde and 9 other chemicals in the exhaled breath of three healthy male laboratory workers. The limit of quantification for formaldehyde was not reported. A series of measurements were taken in the nose and mouth, and also in the oral cavity during breath holding. Table 3-6 presents the median formaldehyde levels and geometric standard deviations for the three subjects. The authors noted that formaldehyde in exhaled breath was at a level somewhat lower than the ambient air concentration, but they could not be certain of its origin.

Table 3-6. Measurements of exhaled formaldehyde concentrations in the mouth and nose, and in the oral cavity after breath holding in three healthy male laboratory workers

Subject		Formaldehyde (median ppb / σg)
A	Mouth	5 / 2.3
	Nose	7 / 2.1
	Oral cavity	5 / 2.3
B	Mouth	7 / 2.3
	Nose	5 / 2.1
	Oral cavity	6 / 1.9
C	Mouth	4 / 2.5
	Nose	6 / 1.9
	Oral cavity	6 / 1.9
Laboratory air		9.6 ±1.5

Source: Wang et al. (2008).

Cáp et al. (2008) evaluated relationships between volatile organic compounds measured in exhaled breath and exhaled breath condensate. Exhaled breath condensate consists of aerosolized particles of airway lining fluid evolved from the airway wall by turbulent airflow that serve as seeds for substantial water vapor condensation, which then serves to trap water soluble volatile gases. This study also attempted to ascertain whether the source of each compound was endogenous or exogenous. According to the published article and electronic communication with Dr. Patrik Španěl, a co-author for this study, the limit of quantification was 3 ppb or better. Measurements of formaldehyde in the direct exhaled breath of 34 subjects (25 to 62 years; 11 males; 2 smokers) varied from 0 to 12 ppb with a mean of 2 ppb and a median of 1 ppb. Measurements of formaldehyde in exhaled breath condensate ranged from 0 to 12 ppb with a mean of 2 ppb and a median of 0 ppb. Two smokers exhaled formaldehyde concentrations of 0 and 3 ppb. The scatter plot in Figure 3-5 shows that most subjects exhaled formaldehyde concentrations of 0-3 ppb (x axis), which was considerably lower than the ambient air concentration of 9.6 ±1.5 ppb. The authors concluded that the exhaled concentrations were influenced by exogenous levels in room air, which were not controlled. Dr. Španěl offered two plausible explanations for why exhaled formaldehyde levels are lower than inhaled levels. He noted that some subjects were tested within several minutes of entering the laboratory from outdoors, so they may not have had time to acclimate to the higher indoor air concentration. Another explanation is that a substantial portion of inhaled formaldehyde, which is highly reactive, was retained in the respiratory tract and thus not exhaled; that is, 9.6 ppb of formaldehyde was inhaled but only a mean of 2 ppb was exhaled.

In this and other human studies, there was no adjustment for an artifact in the analytical method that makes it impossible to distinguish between formaldehyde and reaction products for 1% of exhaled methanol and ethanol because they have the same mass to charge ratio (*m/z* = 31). In fact, the concentration of methanol and ethanol that is misidentified as formaldehyde exceeds the reported concentrations of exhaled formaldehyde. Thus, it is highly likely that the actual exhaled formaldehyde concentration in Cáp et al. (2008) was significantly lower than 2 ppb, and that there was little or no endogenous formaldehyde in the exhaled breath. This would be consistent with an animal study in which Mashford and Jones (1982) detected no exhaled formaldehyde in rats injected I.P. with 40 mg/kg [^{14}C]-formaldehyde. Over 48 hours, 78% of the radioactivity was exhaled as $^{14}CO_2$ and 11% was excreted in the urine as formate, N-(hydroxymethyl)urea, N,N'-bis-(hydroxymethyl)urea, and possibly polymethylene urea. In summary, there are insufficient data at this time to confidently establish a concentration of formaldehyde in exhaled breath that can be attributed to endogenous sources.

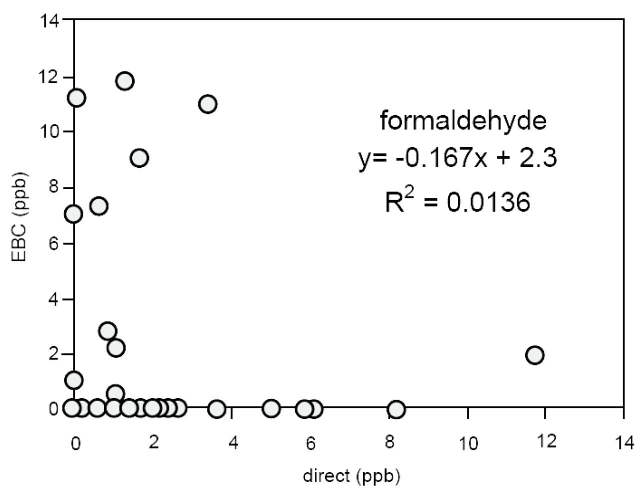

Figure 3-5. Scatter plot of formaldehyde concentrations measured in ppb in direct breath exhalations (x axis) and exhaled breath condensate headspace (y axis).

Source: Cáp et al. (2008).

3.5.3. Formaldehyde Excretion in Human Urine

Gottschling et al. (1984) examined urinary formic acid in 35 veterinary students. Personal monitoring badges were worn and returned after class, and urine samples were taken prior to class and within 2 hours after the class. Mean exposure levels were about 100 ppb. Baseline averages of urinary formic acid (as a sodium salt) were 12.47 mg/L and ranged from 2.43 to 28.38 mg/L among subjects. Postexposure formate levels were slightly elevated but were not statistically significant. Moreover, formate levels decreased in several individuals relative to pre-exposure levels. The authors concluded that variability in urinary formate may mask any changes and that monitoring formate within 2 hours of exposure is not informative. It is worth noting, however, that interpretation of this finding is confounded due to the fact that diet was not controlled and because no markers for urinary normalization were employed (Boeniger, 1987).

Boeniger (1987) reviewed previously published data on formate in urine (some of which were in German). In one occupational study, workers were exposed to an average formaldehyde exposure of 1.28 mg/m^3 over a 6-hour work shift. This implies an average intake of 6 mg;[6] Boeniger reported a range of 2.5 to 13 mg. However, the original study reported that post-shift formate levels were 152 mg/L, whereas the levels were only 24 mg/L 6 days later (no exposure). Considering that only a small percentage of inhaled formaldehyde would be excreted in urine, it is unclear how (or whether) formaldehyde exposure, with the highest total dose of 13 mg, could be responsible for the observed increase.

In the previously described study by Shin et al. (2007), human urine samples were shown to contain TZCA, although variability was not reported. A subsequent study reported that urine TZCA levels were higher in individuals living in newer apartments (0.18 ± 0.121 mg/g creatinine) as compared to older apartments (0.097 ± 0.040 mg/g creatinine) (Li et al., 2007)[7]. The authors cited this as evidence that TZCA is a urinary marker for formaldehyde exposure, even though TZCA levels were not correlated to measured (or estimated) formaldehyde exposures. The individuals also differed significantly in age (21.5 vs. 28.6, $p = 0.053$) and differed in smoking percentage (10 vs. 27%). Clearly these two studies do not establish a relationship between human formaldehyde exposure and urine TZCA levels.

3.6. MODELING THE TOXICOKINETICS OF FORMALDEHYDE AND DPX

3.6.1. Motivation

Airway geometry is expected to be an important determinant of inhaled formaldehyde dosimetry in the respiratory tract and its differences across species. The uptake of formaldehyde in the upper respiratory tract is highly nonhomogenous and spatially localized and exhibits strong species differences. Species differences in kinetic factors have been argued to be the key

[6] 1.28 mg/m^3 / 1,000L/m^3 × 13.8L/minute × 60 minutes/hour × 6 hours.

[7] This study is described in greater detail in Chapter 5.

determinants of species-specific lesion distributions for formaldehyde and other reactive inhaled gases. In the first subsection here, the advantage gained in the quantitative risk assessment by modeling these differences in the upper respiratory tract is explained. Such a model was constructed by using computational fluid dynamic (CFD) methods for modeling airflow and regional formaldehyde uptake in the rat, rhesus monkey, and human nose by scientists at the Chemical Industries Institute of Toxicology (CIIT) Centers for Health Research (presently the Hamner Institutes of Health Sciences). While frank effects were seen only in the upper respiratory tract in rodents, mild lesions were also present in the major bronchiolar region of the rhesus monkey. Therefore, with regard to extrapolation of cancer risk from animal bioassays to humans, the upper and lower human respiratory tract should both be considered potentially at risk of developing formaldehyde-induced squamous cell carcinoma. Therefore, formaldehyde dose to the entire human respiratory tract human respiratory tract was modeled in order to develop a dose-response relationship that considered the entire respiratory tract. Accordingly, in the second subsection results of modeling airflow and regional formaldehyde uptake in the human lower respiratory tract by Overton et al. (2001) are provided. Unsteady effects were argued to be insignificant at resting breathing rates, and therefore steady-state inspiratory flow was assumed. Since these models have been described in various reports and publications, the technical details are consigned to appendices or the literature is referenced.

The fluid dynamics modeling in the respiratory tract comprises two steps (Kimbell et al. 2001): airflow through the lumen and formaldehyde uptake by the lining of the respiratory tract. Flow streamlines in the CFD simulations agreed reasonably well with experimentally observed patterns in casts of the rat, monkey, and human nasal passages as well as with measurements of velocity taken in hollow molds of the human nose. Pressure drop as a function of volumetric flow also compared well with measurements made in rats. Unlike the airflow simulations, no validation of the regional formaldehyde uptake simulations (that is, the spatial distribution of uptake) was possible. (It was possible to compare simulations of overall uptake with experimentally observed values.) In this assessment, several indirect qualitative and quantitative lines of evidence were relied on to provide general confidence in the formaldehyde regional uptake profile in the F344 rat nasal passages. In addition to the agreement mentioned earlier with respect to airflow profiles, this evidence includes general agreement between measured and predicted levels of formaldehyde DPXs (in the “high-tumor” regions) when simulations of airflow and regional formaldehyde uptake were used as input to a physiologically based pharmacokinetic (PBPK) model for DPX kinetics (Cohen-Hubal et al. 1997). Such indicators are not available for the simulation of uptake patterns in the human. With regard to modeling the lower respiratory tract, calculations in Overton et al. (2001) are based on an idealized representation of airways in the human lung and of air flow through them (referred to in the literature as “single-path” models). Overton et al. (2001) did not attempt to validate their simulations. However, the following observation may be noted in support of their model. In the case of the deposition of coarse and fine particulate matter, single-path models have traditionally provided a reasonably accurate representation of the average deposition in a given generation of the lung airways (i.e. airways at a given depth in the lung) for a normal human population.

There were mass balance errors in the CFD calculations (Kimbell et al. 2001). Mass balance errors associated with formaldehyde uptake into tissue ranged from less than 14% for the rat, monkey, and human at resting minute volume to approximately 27% at the highest inspiratory flow rates of 31.8 and 37 L/minute in the human.

If DPX formation and cell proliferation are driven by formaldehyde flux, then these quantities may also be expected to exhibit site and species differences, thus arguing for linking these quantities to the modeled formaldehyde flux (Conolly et al. 2000).

The third subsection evaluates PBPK models for DPX kinetics in the F344 rat and rhesus monkey, using CFD simulations of formaldehyde flux to the nasal lining as input (Klein et al., 2009; Subramaniam et al., 2007; Conolly et al., 2000), and discusses their uncertainties. This subsection further discusses issues related to the scaling of the animal models to the human.

This assessment uses internal dose metrics computed by using the models described in this section so as to derive more accurate human equivalent concentrations from the animal bioassays than would be obtained by averaging over the respiratory surface area. The strengths and uncertainties associated with the data and the models and their relevance to the hypothesized mode of action are discussed in some length.

3.6.2. Species Differences in Anatomy: Consequences for Gas Transport and Risk

As discussed earlier, formaldehyde is highly reactive and water soluble (categorized as a category 1 gas), thus its absorption in the mucus layer and tissue lining of the upper respiratory tract is known to be significant. The regional inhaled dose of formaldehyde to the respiratory tract of a given species depends on the amount of formaldehyde delivered by inhaled air, the absorption characteristics of the nasal lining, and reactions in the tissue. The amount delivered by inhaled air is a function of the major airflow patterns, air-phase diffusion, and absorption at the airway-epithelial tissue interface. The dose of formaldehyde to the epithelial tissue, which is different from the amount delivered, depends on the amount absorbed at the airway-tissue interface, water solubility, mucus-to-tissue phase diffusion, and chemical reactions, such as hydrolysis, protein binding, and metabolism. It has been argued strongly that species differences in these kinetic factors are determinants of species-specific lesion distributions for formaldehyde and other inhaled gases (Moulin et al., 2002; Bogdanffy et al., 1999; Ibanes et al., 1996; Monticello et al., 1996; Monticello and Morgan, 1994; Morgan et al., 1991).

Because of the convoluted nature of the airways in the upper respiratory tract, the absorption of such gases in the upper respiratory tract is highly nonhomogeneous. There are large differences across species in the anatomy of the upper respiratory tract (Figure 3-6) and in airflow patterns (Figure 3-7). Therefore, as shown in the simulations in Figure 3-8, it may be expected that the uptake patterns and thus risk due to inhaled formaldehyde will also show strong species dependence. Morgan et al. (1991) concluded that airflow-driven dosimetry plays a critical role in determining the site specificity of various formaldehyde-induced responses, including tumors, in the nose of the F344 rat. The convoluted geometry of the airway passages in the upper respiratory tract, as seen from the cross sections of the nose in Figure 3-6, renders an idealized representation of fluid flow and uptake profiles almost impossible. For these reasons, Kimbell et al. (1993), Kepler et al. (1998), and Subramaniam et al. (1998) developed anatomically realistic finite-element representations of the noses of humans, F344 rats, and rhesus monkeys. These representations were subsequently used in physical and computational models (Figure 3-6). This assessment utilizes dosimetry derived from these representations.

An accurate calculation of species differences in formaldehyde dosimetry in the upper respiratory tract is important to the extrapolation problem for another reason. The upper respiratory tract in rats is an extremely efficient scrubber of reactive gases (97% uptake) (Morgan et al., 1986), thereby protecting the lower respiratory tract from gaseous penetration. On the other hand, there is considerably more fractional penetration of formaldehyde into the lower respiratory tract of the rhesus monkey than in the rat (see Figure 3-8). Therefore, an accurate determination of scrubbing in the upper respiratory tract is important to delineate species differences in the level of risk to the lower respiratory tract. Thus, in the case of the rhesus monkey, the model by Kepler et al. (1998) included the trachea. Because the human model also had to address the potential for oronasal breathing, an idealized single-path model of the lower respiratory tract was attached to a model of the upper respiratory tract (Overton et al., 2001). It is important to note that the models mentioned above represent nasal passages reconstructed from a single individual from each species (Kimbell et al., 2001a, b; Conolly et al., 2000; CIIT, 1999; Subramaniam et al., 1998). This is discussed later in the context of intraspecies variability.

The highly localized nature of uptake patterns shown in Figure 3-8 means that averaging uptake over the entire nasal surface area would dilute the regional dose over areas where response was observed and that an extrapolation based on such averaging would clearly not be accurate.

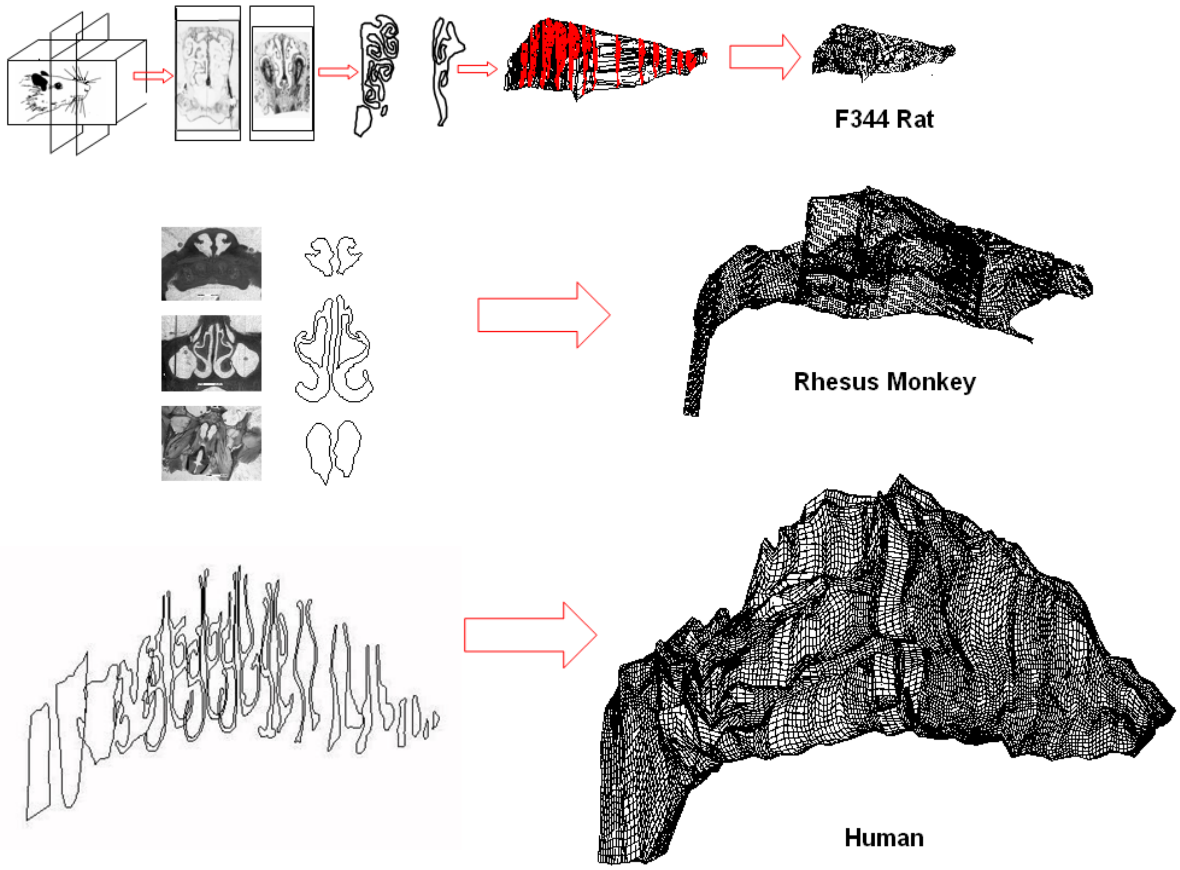

Figure 3-6. Reconstructed nasal passages of F344 rat, rhesus monkey, and human.

Note: Nostril is to the right, and the nasopharynx is to the left. Right side shows the finite element mesh. Left-hand side shows tracings of airways obtained from cross sections of fixed heads (F344 rat and rhesus monkey) and magnetic resonance image sectional scans (humans). Aligned cross sections were connected to form a three-dimensional reconstruction and finite-element computational mesh. Source: Adapted from Kimbell et al. (2001a). Additional images provided courtesy of Dr. J.S. Kimbell, CIIT Hamner Institutes.

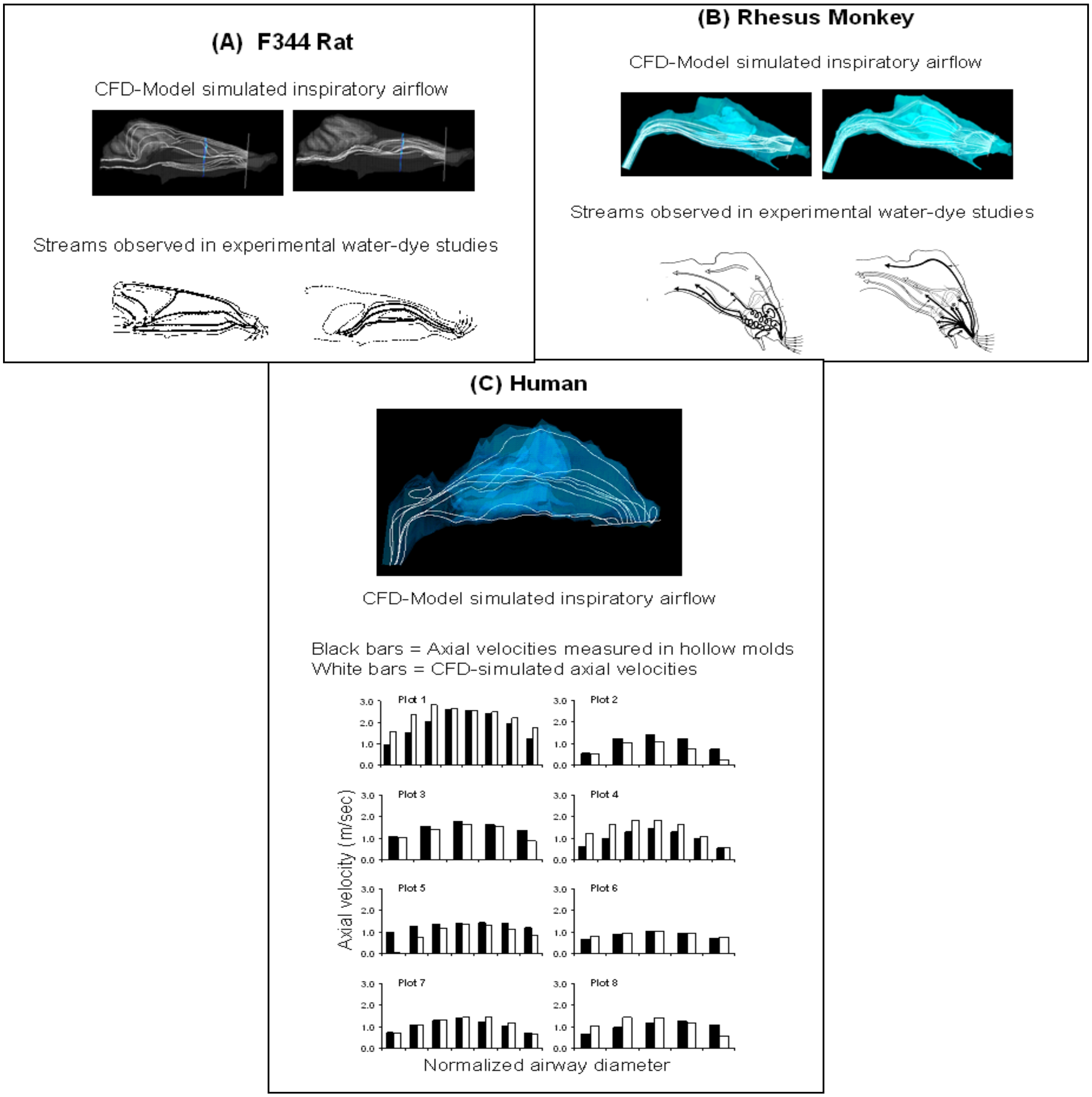

Figure 3-7. Illustration of interspecies differences in airflow and verification of CFD simulations with water-dye studies.

Note: Panels A and B show the simulated airflow pattern versus water-dye streams observed experimentally in casts of the nasal passages of rats and monkeys, respectively. Panel C shows the simulated inspiration airflow pattern, and the histogram depicts the simulated axial velocities (white bars) vs. experimental measurements made in hollow molds of the human nasal passages. Dye stream plots were compiled for the rat and monkey over the physiological range of inspiration flow rates. Modeled flow rates in humans were 15 L/minute.

Source: Adapted from Kimbell et al. (2001a).

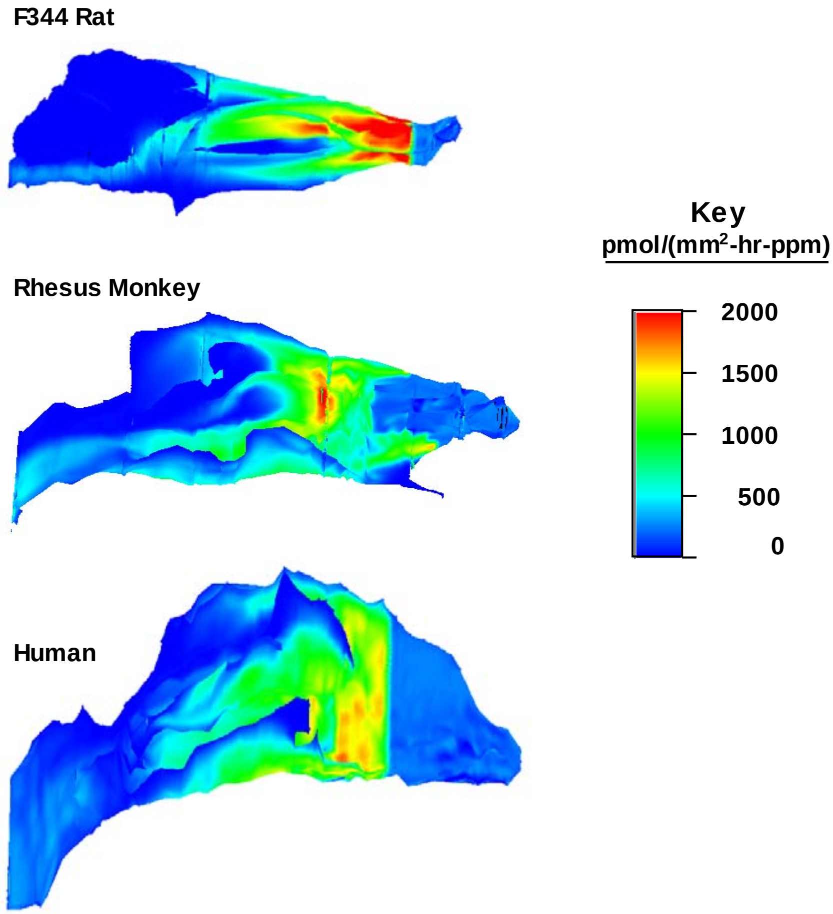

Figure 3-8. Lateral view of nasal wall mass flux of inhaled formaldehyde simulated in the F344 rat, rhesus monkey, and human.

Note: Nostrils are to the right. Simulations were exercised in each species at steady-state inspiration flow rates of 0.576 L/minute in the rat, 4.8 L/minute in the monkey, and 15 L/minute in the human. Flux was contoured over the range from 0–2,000 pmol/(mm^2-hour-ppm) in each species.

Source: Kimbell et al. (2001a).

Another factor to consider in the extrapolation is that monkeys and humans are oronasal breathers while rats are obligate nose-only breathers. Thus, for humans and monkeys, oronasal or oral breathing implies a significantly higher uptake in the lower respiratory tract. It is known that a significant fraction of the human population breathes normally through the mouth. Finally, activity profiles are also determinants of extraction efficiency (see Figure 3-9) and of breathing route (Niinimaa et al., 1981). Given the fact that formaldehyde-induced lesions were observed as far down the respiratory tract as the first bifurcation of the lungs in exposed monkeys, the entire human respiratory tract should be considered when extrapolating data from rats.

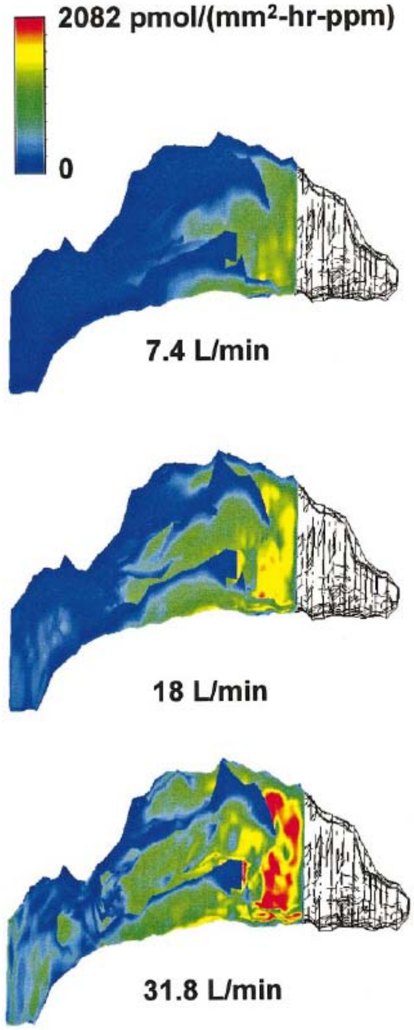

Figure 3-9. CFD simulations of formaldehyde flux to human nasal lining at different inspiratory flow rates.

Note: Right lateral view. Uptake is shown for the non-squamous portion of the epithelium. The front portion of the nose (vestibule) is lined with keratinized squamous epithelium and is expected to absorb relatively much less formaldehyde.

Source: Kimbell et al. (2001b).

3.6.3. Modeling Formaldehyde Uptake in Nasal Passages

CIIT scientists chose the F344 strain of the rat since it was assumed to be anatomically representative of its species and because it is widely used experimentally, most notably in bioassays sponsored by the National Toxicology Program and at CIIT. The approximate locations of squamous, mucus-coated, and nonmucus epithelial cells were mapped onto the reconstructed nasal geometry of the CFD models. Taken together, these regions of nonmucus and mucus-coated cells comprise the entire surface area of the nasal passages (see original papers and CIIT [1999] for further details on reconstruction and morphometry). Types of nasal epithelium overlaid onto the geometry of the models were assumed to be similar in characteristics across all three species (rat, monkey, and human) except for thickness, surface area, and location. Species-specific mucosal thickness, surface area, and location were estimated from the literature, from the documentation of the CFD models, or by direct measurements (Conolly et al., 2000; CIIT, 1999). The nasal passages of all three species were assumed to have a continuous mucus coating over all surfaces except specific areas in the nasal vestibule. As discussed at the beginning of this chapter, formaldehyde hydrolyzes in water and reacts readily with a number of components of nasal mucus. Absorption rates of inhaled formaldehyde by the nasal lining were therefore assumed to depend on where the epithelial lining is coated by mucus and where it is not.

To calculate an airflow rate that would be comparable among species, the amount of inspired air (tidal volume, V_T) was divided by the estimated time involved in inhalation (half the time a breath takes, or (1/2)(1/[breathing frequency, f]). Thus, an inspiratory flow rate was calculated to be $2V_Tf$, or twice the minute volume. Predicted flux values represent an average of one nasal cycle. Minute volumes were allometrically scaled to 0.288 L/minute for a 315 g rat from data given by Mauderly (1986). Simulations were therefore carried out at 0.576 L/minute for the rat.

The fluid dynamics modeling in the respiratory tract comprises two steps: modeling the airflow through the lumen (solution of Navier-Stokes equations) and modeling formaldehyde uptake by the respiratory tract lining (solution of convective-diffusion equations for a given airflow field). Details of these simulations, including boundary conditions for air flow and mass transfer, are provided in Kimbell et al. (2001a, b, 1993) and Subramaniam et al. (1998). Formaldehyde absorption at the airway-to-epithelial tissue interface was assumed to be proportional to the air-phase formaldehyde concentration adjacent to the nasal lining layer in monkeys and humans (see the original paper [Kimbell et al., 2001a] for a more detailed elaboration of the calculations for these coefficients).

Because formaldehyde is highly water soluble and reactive, Kimbell at al. (2001a) assumed that absorption occurred only during inspiration. Thus, for each breath, flux into nasal passage walls (rate of mass transport in the direction perpendicular to the nasal wall per mm^2 of the wall surface) was assumed to be zero during exhalation, with no backpressure to uptake built up in the tissues. Overton et al. (2001) estimated the error due to this assumption to be small, roughly an underestimate of 3% in comparison to cyclic breathing. Also, this assumption is the same as that used in default methods for reference concentration determination and has been used in other PBPK model applications to describe nasal uptake (Andersen and Jarabek, 2001).

3.6.3.1. *Flux Bins*

A novel contribution of the CIIT biologically motivated dose-response model is that cell division rates and DPX concentrations are driven by the local concentration of formaldehyde. These were determined by partitioning the nasal surface by flux, resulting in 20 “flux bins.” Each bin was comprised of elements (not necessarily contiguous) of the nasal surface that receive a particular interval of formaldehyde flux per ppm of exposure concentration (Kimbell et al., 2001a). The spatial coordinates of elements comprising a particular flux bin were fixed for all exposure concentrations, with formaldehyde flux in a bin scaling linearly with exposure concentration (ppm). Thus, formaldehyde flux was expressed as pmol/(mm^2-hour-ppm).

3.6.3.2. *Flux Estimates*

Formaldehyde flux was estimated for the rat, monkey, and human over the entire nasal surface and over the portion of the nasal surface that was lined by nonsquamous epithelium. Formaldehyde flux was also estimated for the rat and monkey over the areas where cell proliferation measurements were made (Monticello et al., 1991, 1989) and over the anterior portion of the human nasal passages that is lined by nonsquamous epithelium. Figure 3-8 shows the mass flux of inhaled formaldehyde to the lateral wall of nasal passages in the F344 rat, rhesus monkey, and human (Kimbell et al., 2001a).

Maximum flux estimates for the entire upper respiratory tract were located in the mucus-coated squamous epithelium on the dorsal aspect of the dorsal medial meatus near the boundary between nonmucus and mucus-coated squamous epithelium in the rat, at the anterior or rostral margin of the middle turbinate in the monkey, and in the nonsquamous epithelium on the proximal portion of the mid-septum near the boundary between squamous and nonsquamous epithelium in the human (see Kimbell et al. [2001b] for tabulations of comparative estimates of formaldehyde flux across the species).

The rat-to-monkey ratio of the highest site-specific fluxes in the two species was 0.98. In the rat, the incidence of formaldehyde-induced squamous cell carcinomas in chronically exposed animals was high in the anterior lateral meatus (Monticello et al., 1996). Flux predicted per ppm in this site and flux predicted near the anterior or proximal aspect of the inferior turbinate and adjacent lateral walls and septum in the human were similar, with a rat-to-human ratio of 0.84.

3.6.3.3. *Mass Balance Errors*

Overall uptake of formaldehyde was calculated as 100% x (mass entering nostril − mass exiting outlet)/(mass entering nostril). Mass balance errors for air, 100% x (mass of air entering nostril − mass exiting outlet)/(mass entering nostril), and inhaled formaldehyde, 100% x (mass entering nostril − mass absorbed by airway walls − mass exiting outlet)/(mass entering nostril), were calculated. Mass balance errors associated with simulated formaldehyde uptake from air into tissue ranged from less than 14% for the rat, monkey, and human at 7.4 and 15 L/minute to approximately 27% at the highest inspiratory flow rates of 31.8 and 37 L/minute (Kimbell et al., 2001b). Kimbell et al. (2001b) corrected the simulation results for these errors by evenly distributing the lost mass over the entire nasal surface.

3.6.4. Modeling Formaldehyde Uptake in the Lower Respiratory Tract

Lesions were observed in the lower respiratory tract of rhesus monkeys exposed to 6 ppm formaldehyde. Therefore it is appropriate to consider the human lower respiratory tract as potentially at risk for formaldehyde-induced cancer. Accordingly, fluid flow and formaldehyde uptake in the lower respiratory tract were also modeled for the human in the CIIT approach by using dosimetry estimates for the human lower respiratory tract.

The single-path idealization of the human lung anatomy captures the geometrical characteristics of the airways for a given lung depth, and of airflow through these airways, in an average, homogeneous sense. For particulates, this has provided a reasonable representation of the average deposition in a given generation of the lung airways for a normal human population. The one-dimensional model by Weibel (1963) is generally considered adequate unless the fluid dynamics at airway bifurcations need to be explicitly modeled. However, such an idealization of the lung geometry has been successfully used in various models for the dosimetry of ozone and particulate and fibrous matter. Most likely, the lung geometries of the susceptible population, such as those with chronic obstructive pulmonary disease, would depart significantly from the geometry described in Weibel (1963). Unlike the accurate representation of the nasal anatomy used in the CFD modeling, the lung geometry is idealized in the CIIT approach as a typical path Weibel geometry. This captures the lung structure in an average, homogeneous sense for a given lung depth. The single-path model used to calculate formaldehyde uptake in the human respiratory tract (Overton et al., 2001; CIIT, 1999) applied a one-dimensional equation of mass transport to each generation of an adult human symmetric, bifurcating Weibel-type respiratory tract anatomical model, augmented by an upper respiratory tract. The detailed CFD modeling of the upper respiratory tract was made consistent with the upper respiratory tract in the single-path model by requiring that the one-dimensional version of the nasal passages have the same inspiratory air-flow rate and uptake during inspiration as the CFD simulations for four daily human activity levels. The reader is referred to Overton et al. (2001) for further details of the simulations. Results most relevant to this assessment are shown in Figure 3-10.

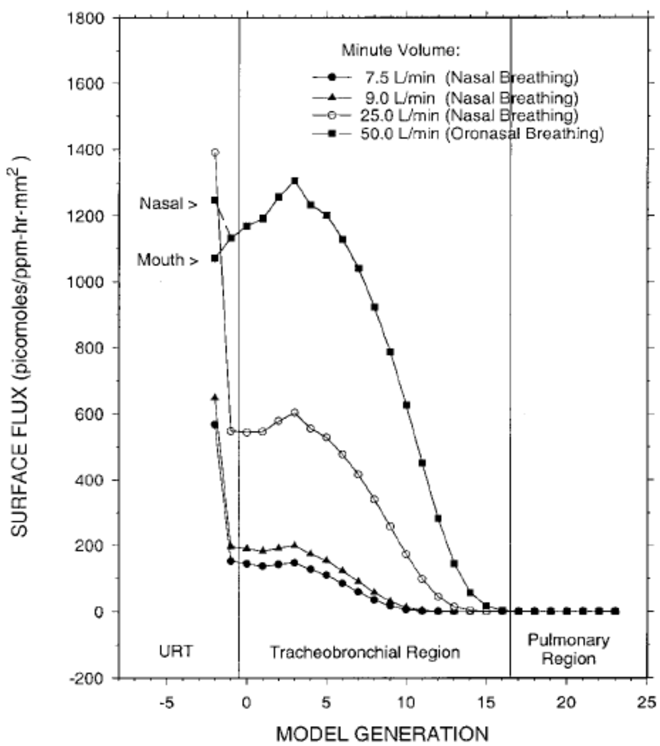

Figure 3-10. Single-path model simulations of surface flux per ppm of formaldehyde exposure concentration in an adult male human.

Source: Overton et al. (2001).

The primary predictions of the model, as shown in Figure 3-10, were that more than 95% of the inhaled formaldehyde would be retained and formaldehyde flux in the lower respiratory tract would increase for several lung airway generations from that in the posterior-most segment of the nose and then decrease rapidly, resulting in almost zero flux to the alveolar sacs.

Overton et al. (2001) modeled uptake at higher inspiratory rates, including those at 50 L/minute of minute volume (well beyond levels where the oronasal switch occurs in the normal nasal breathing population). At these rates Figure 3-8 indicates that formaldehyde flux in the mouth cavity is comparable (but a bit less) to that occurring in the nasal passages. Overton et al. (2001) did not model uptake in the oral cavity at minute volumes less than 50 L/minute. This would be of interest because mouth breathers form a large segment of the population. Furthermore, at concentrations of formaldehyde where either odor or sensory irritation becomes a significant factor, humans are likely to switch to mouth breathing even at resting inspiration. At a minute volume of 50 L/minute, Overton et al. (2001) assumed, citing Niinimaa et al. (1981), that 0.55 of the inspired fraction is through the mouth. Therefore, based on the results in Figure 3-8, it is not unreasonable to assume that for mouth breathing conditions at resting or light exercise inspiratory rates, average flux across the human mouth lining would be comparable to the average flux across the nasal lining computed in Kimbell et al. (2001a, b).

3.6.5. Uncertainties in Formaldehyde Dosimetry Modeling

3.6.5.1. *Verification of Predicted Flow Profiles*

The simulated streamlines of steady-state inspiration airflow predicted by the CFD model agreed reasonably well with experimentally observed patterns of water-dye streams made in casts of the nasal passages for the rat and monkey as shown in panels A and B in Figure 3-7. The airflow velocity predicted by CFD model simulations of the human also agreed well with measurements taken in hollow molds of the human nasal passages (panel C, Figure 3-8) (Kepler et al., 1998; Subramaniam et al., 1998; Kimbell et al., 1997, 1993). However, the accuracy and relevance of these comparisons are limited. The profiles were verified by video analysis of dye streak lines in the molds of rats and rhesus monkeys, although this method is reasonable for only the major airflow streams.

Plots of pressure drop vs. volumetric airflow rate predicted by the CFD simulations compared well with measurements made in rats in vivo (Gerde et al., 1991) and in acrylic casts of the rat nasal airways (Cheng et al., 1990) as shown in Figure 3-11. This latter comparison remains qualitative due to differences among the simulation and experiments as to where the outlet pressure was measured and because no tubing attachments or other experimental apparatus were included in the simulation geometry. The simulated pressure drop values were somewhat lower, possibly due to these differences.

Inspiratory airflow was assumed to be constant in time (steady state). Subramaniam et al. (1998) considered this to be a reasonable assumption during resting breathing conditions based on a value of 0.02 obtained for the Strouhal number. Unsteady effects are insignificant when this number is much less than one. However, this assumption may not be reasonable for light and heavy exercise breathing scenarios.

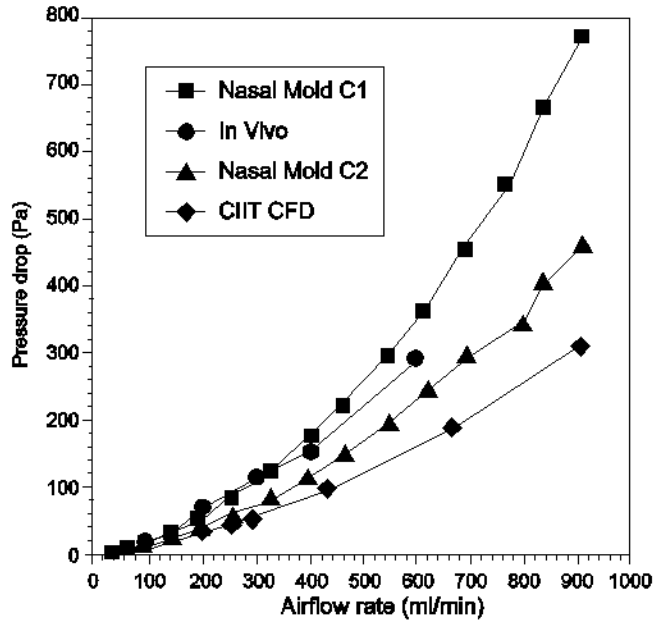

Figure 3-11. Pressure drop vs. volumetric airflow rate predicted by the CIIT CFD model compared with pressure drop measurements made in two hollow molds (C1 and C2) of the rat nasal passage (Cheng et al., 1990) or in rats in vivo (Gerde et al., 1991).

Source: Kimbell et al. (1997).

3.6.5.2. *Level of Confidence in Formaldehyde Uptake Simulations*

Unlike the airflow simulations, it was not possible to evaluate the formaldehyde uptake calculations directly. Since the mass transfer boundary conditions were set by fitting overall uptake to the average experimental data for various exposure concentrations, it was not possible to independently verify even the overall uptake values with empirical data. This assessment has relied on several indirect qualitative and quantitative lines of evidence listed below to provide general confidence in the uptake profile for the F344 rat nasal passages, as modeled in CIIT (1999), when gross averages are considered over certain regions of the nasal lining.

In an earlier simulation, where the nasal walls were set to be infinitely absorbing of formaldehyde, uptake of inhaled formaldehyde in the upper respiratory tract was predicted to be 90% in the rat for simulations corresponding to the resting minute volume in the F344 rat. This estimate compared reasonably well with the range of 91–98% observed by Morgan et al. (1986a).

Morgan et al (1991) showed general qualitative correspondence between the main routes of flow and lesion distribution induced by formaldehyde in the rat nose. In their initial work with a CFD model that represented a highly reactive and soluble gas, Kimbell et al. (1993) described similarities in computed regional mass flux patterns and lesion distribution due to formaldehyde. When the results from this work in the coronal section immediately posterior to the vestibular region were considered, simulated flux levels over regions such as the medial aspect of the maxilloturbinate and the adjacent septum (where lesions were seen) were an order of magnitude higher than over other regions, such as the nasoturbinate (where lesions were not seen).[8]

The results of a PBPK model by Cohen-Hubal et al. (1997) provide a reasonable level of confidence in regional uptake simulations for the F344 rat when gross averages over nasal sites are carried out. Cohen-Hubal et al. (1997) linked the CFD dosimetry model for formaldehyde to a PBPK model for formaldehyde-DPX concentration in the F344 rat. This PBPK model was calibrated by optimizing the model to combined DPX data from high-tumor incidence and low-tumor incidence regions of the rat nose that were obtained in separate experiments by Casanova et al. (1991, 1989). These data were obtained at 0.3, 0.7, 2.0, 6.0, and 10 ppm for both regions and also at 15 ppm for the high-tumor region. Model prediction of DPX concentrations for the high-tumor region only compared well with the experimental data, including 15 ppm for which the model had not been calibrated. This is shown in Figure 3-12.

The CFD simulations do not model reflex bradypnea, a protective reflex seen in rodents but not in humans. As discussed at length in sections 3.2.3.1 and 4.2.1.1, it is reasonable to expect a range of 25% (Chang et al., 1983) to 45% (Barrow et al., 1983) decrease in minute volume in F344 rats at the exposure concentration of 15 ppm. Explicit omission of this effect in the modeling is, however, not likely to be a source of major uncertainty in the modeled results for uptake of formaldehyde in the rat nose for the following reason. The CFD model for the F344 rat was calibrated to fit the overall experimental result for formaldehyde uptake in the F344 rat at 15 ppm exposure concentration. This was carried out by adjusting the mass transfer coefficient used as boundary condition on the absorbing portion of the nasal lining. Thus, the reflex bradypnea occurring in those experimental animals is phenomenologically factored into the value used for the boundary condition. Nonetheless, some error in the localized distribution of uptake patterns may be expected, even if the overall uptake is reproduced correctly.

---

[8] However, this 1993 CFD model differed somewhat from the subsequent model by Kimbell et al. (2001a) used in this assessment. In the 1993 model, the limiting mass-transfer resistance for the gas was assumed to be in the air phase; that is, the concentration of formaldehyde was set to zero at the airway lining. Furthermore, this same boundary condition was used on the nasal vestibule as well, while, in the more recent model, the vestibule was considered to be non-absorbing. Unfortunately, Kimbell at al. (2001a) did not report on correspondences between

Furthermore, since the same value for the mass transfer coefficient was used in human simulations (as obtained from calibration of the rat model), there is additional uncertainty in the modeled human flux estimates. This issue was not addressed by Kimbell et al. (2001a, b), Conolly et al. (2004), or Schlosser et al. (2003), and we are unable to assess the extent of this error more accurately.

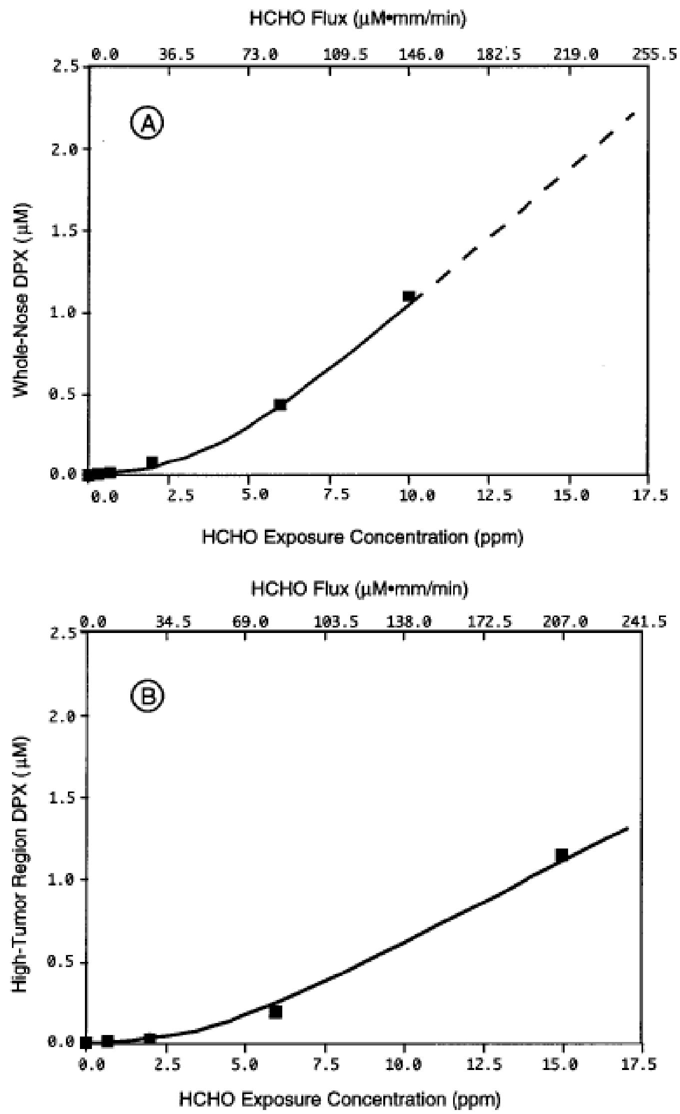

Figure 3-12. Formaldehyde-DPX dosimetry in the F344 rat.
Panel A: calibration of the PBPK model using data from high and low tumor incidence sites. Panel B: model prediction compared against data from high tumor incidence site. Dashed line in panel A shows the extrapolation outside the range of the calibrated data.
Source: Cohen-Hubal et al. (1997).

flux patterns and lesion distribution.

3.6.6. PBPK Modeling of DNA Protein Cross-Links (DPXs) Formed by Formaldehyde

3.6.6.1. *PBPK Models for DPXs*

As can be seen from the previous sections, measuring the distribution of the absorbed formaldehyde and identifying its form have proven difficult. Because of the high reactivity of formaldehyde, rapid metabolism of formaldehyde, and complexity of formate clearance, dose surrogates (or biomarkers) of exposure have been used to characterize the extent of absorption and distribution of formaldehyde. As with other soluble and reactive gases, typical PBPK models that predict steady-state blood concentrations are not useful for predicting formaldehyde dosimetry at this time. As noted previously, inhalation exposure to formaldehyde has not been shown to increase blood formaldehyde levels. Thus, most modeling efforts for formaldehyde have focused on disposition at the site of contact.

As discussed earlier, the concentration of DPXs formed by formaldehyde has been treated as a surrogate for the tissue dose of formaldehyde in earlier efforts by Casanova et al. (1991) and in EPA's efforts to update its health assessment of formaldehyde (Hernandez et al., 1994). These efforts used data from rats and rhesus monkeys (Casanova et al., 1991, 1989). Using DPXs in this manner allowed the incorporation of both clearance and metabolism of formaldehyde and the incorporation of the effect of saturation on detoxification of formaldehyde at higher doses. Calculation of the average DPX concentration from these data was seen as a surrogate for the area under the curve (AUC) of the reactive formaldehyde species in the epithelium. Based on these data, Casanova et al. (1991) developed a PBPK model for predicting DPXs in these species and for extrapolating to the human.

The Casanova et al. (1991) model consists of three anatomical compartments representing different parts of the upper respiratory tract of the rhesus monkey. The results indicated a 10-fold difference in DPX formation between rats and monkeys, due primarily to species differences in minute volume and differing quantities of DNA in the nasal mucosa. Casanova et al. (1991) then developed a monkey/rat scaling factor for these parameters by taking the ratio of nasal mucosa tissue between the two species, a determinant that was proportional to the total body weight differences between the two species. Using these scaling factors in their model, the authors' predictions in monkey (based on the rat data) were in close agreement with observed DPXs in monkey, particularly at higher formaldehyde concentrations. However, the model overpredicted DPX formation in the monkey at lower formaldehyde concentrations. Subsequent rat-human and monkey-human scaling results predicted much lower DPX formation in man. Again, the values obtained at lower concentrations may have been overpredicted, as was the case for rat-monkey extrapolation.

Georgieva et al. (2003) developed a model for the uptake and disposition of formaldehyde in the rat nasal lining. This model was designed to predict the distribution of formaldehyde in the nasal mucosa. The model indicated that, at 6 ppm exposure, a steady-state elevation of 15–20 µM formaldehyde would be achieved within 30 seconds. Furthermore, this same elevation was predicted when the exposure was 6 ppm formaldehyde for 60 minutes. Given that human blood formaldehyde levels are predicted to be about 100 ± 15 µM (Heck et al., 1985) and assuming that blood formaldehyde concentration is roughly equivalent to the concentration predicted at the basement membrane of the epithelium, this model predicts roughly a 15–20% increase in blood formaldehyde. However, it should be noted that a 40-minute inhalation exposure of humans to 1.99 ppm formaldehyde did not lead to a measurable increase in blood formaldehyde (Heck et al., 1985).

Franks (2005) published a mathematical model for predicting the disposition of formaldehyde in the human nasal mucosa and blood. The calculated concentrations of formaldehyde in the mucus, the epithelium, and the blood attained steady-state profiles within a few seconds of exposure. The increase of the formaldehyde concentration in the blood was predicted to be insignificant compared with the existing pre-exposure levels in the body: an increase of 0.00044 mg/L in blood formaldehyde following exposure to 1.9 ppm formaldehyde for up to 8 hours. The model described formaldehyde concentration gradients across the mucus, epithelial, and submucosal compartments in the human nose. Transport of formaldehyde was governed by the following processes: diffusional (in the mucus); a combination of diffusional, two first order terms representing intrinsic reactivity of formaldehyde and binding to DNA, and Michaelis-Menten kinetics representing enzymatic metabolism (in the epithelial layer); a first-order term representing non-enzymatic removal governed by the blood perfusion rate (in the submucosal compartment). The model used the values for the first order reaction rate constants and the Michaelis-Menten parameters (V_{max} and K_m) estimated by Conolly et al. (2000) in their model for extrapolating the rat and rhesus monkey data to the human. The modeling in Franks (2005) was not calibrated or validated against experimental data, but the predictions of negligible penetration of free formaldehyde to the blood are qualitatively in agreement with the conclusions in Heck et al. (1985).

Following the efforts by Casanova and co-workers, Cohen-Hubal et al. (1997), Conolly et al. (2000), and Georgieva et al. (2003) developed models that linked local formaldehyde flux from CFD models to DPX predictions. The focus here will be on the Conolly et al. (2000) effort for the following two reasons: it explicitly incorporates regional formaldehyde dosimetry in the nasal lining by using results from CFD modeling of airflow and gas uptake and it brings data across species (rat and rhesus monkey) to bear on model calibration, such a situation being relatively rare in chemical health risk assessments.

3.6.6.2. *A PBPK Model for DPXs in the F344 Rat and Rhesus Monkey that Uses Local Tissue Dose of Formaldehyde*

In earlier risk assessment efforts (Hernandez et al., 1994; Casanova et al., 1991; U.S. EPA, 1991b), the average DPX concentration was considered a surrogate tissue dose metric for the AUC of the reactive formaldehyde species. Conolly et al. (2003) assigned a more specific role for DPXs, treating local DPX concentration as a dose surrogate indicative of the intercellular concentration of formaldehyde, leading to formaldehyde-induced mutations. These authors indicated that it was not known whether DPXs directly induced mutations (Conolly et al., 2003; Merk and Speit, 1998). This is discussed in detail in the mode-of-action sections in this document. The Conolly et al. (2000) model for the disposition of inhaled formaldehyde gas and DPX in the rat and rhesus nasal lining is relatively simple in terms of model structure because it consists of a single well-mixed compartment for the nasal lining as follows:

1. Formaldehyde flux to a given region of the nasal lining is provided as input to the modeling and is obtained in turn as the result of a CFD model. This flux is defined as the amount of formaldehyde delivered to the nasal lining per unit time per unit area per ppm of concentration in the air in a direction transverse to the airflow. It is locally defined as a function of location in the nose and the inspiratory flow rate and is linear with exposure concentration.
2. The clearance of formaldehyde from the tissue is modeled as follows:
    a. a saturable pathway representing enzymatic metabolism of formaldehyde, which is primarily by formaldehyde dehydrogenase (involving Michaelis-Menten parameters V_{max} and K_m)
    b. a separate first-order pathway, which is assumed to represent the intrinsic reactivity of formaldehyde with tissue constituents (rate constant k_f)
    c. first-order binding to DNA that leads to DPX formation (rate constant k_b)
3. The clearance or repair of this DPX is modeled as a first order process (rate constant k_{loss}).

DPX data

DPX concentrations were estimated from a study by Casanova et al. (1994) in which rats were exposed 6 hours/day, 5 days/week, plus 4 days for 11 weeks to filtered air (naive) or to 0.7, 2, 6, or 15 ppm (0.9, 2.5, 7.4, or 18 mg/m^3) formaldehyde (pre-exposed). On the 5th day of the

12th week, the rats were then exposed for 3 hours to 0, 0.7, 2, 6, or 15 ppm ^{14}C-labeled formaldehyde (with pre-exposed animals exposed to the same concentration as during the preceding 12 weeks and 4 days). The animals were sacrificed and DPX concentrations determined at two sites in the nasal mucosa. Conolly et al. (2000) used these naive rat data to develop a PBPK model that predicted the time-course of DPX concentrations as a function of formaldehyde flux at these sites.[9]

3.6.6.3. *Uncertainties in Modeling the Rat and Rhesus DPX Data*

3.6.6.3.1. ***Half-life of DPX repair.*** In the development of the PBPK model for DPXs, Conolly et al. (2000) assumed a value of 6.5×10^{-3} minute^{-1} for k_{loss}, the first-order rate constant for the clearance (repair) of DPXs, such that the DPXs predicted at the end of a 6-hour exposure to 15 ppm were reduced to exactly the detection limit for DPXs in 18 hours (the period between the end of 1 day's 6-hour exposure and the beginning of the next). This determination of rapid clearance was based on an observation by Casanova et al. (1994) that the DPX concentrations observed in the pre-exposed animals were not significantly higher than those in naïve animals (in which there was no significant DPX accumulation). However, in vitro data (Quievryn and Zhitkovich, 2000) indicate a much slower clearance, with an average k_{loss} of 9.24×10^{-4} minute^{-1}.

Subramaniam et al. (2007) examined the Casanova et al. (1994) data and argued that there was a significantly decreased (~ 40%) level of DPXs in high tumor regions of pre-exposed animals vs. naive animals at 6 and 15 ppm and that the weight of the tissues dissected from those regions increased substantially, indicating a thickening of the tissues. After testing the outcome of changing the tissue thickness in the PBPK model for DPXs, it was apparent to these authors that such a change alone could not account for the dramatic reduction in DPX levels after pre-exposure, even with the higher value of k_{loss} used by Conolly et al. (2000). Therefore, in addition to the gross increase in tissue weight, these data indicated either an induction in the activity of enzymes that remove formaldehyde (aldehyde and formaldehyde dehydrogenase) or other changes in the biochemical properties of the highly exposed tissue that must have occurred. Given such a change, Subramaniam et al. (2007) concluded that the experimental results in Casanova et al. (1994) were consistent with the smaller experimental value of k_{loss} indicated by the Quievryn and Zhitkovich (2000) data. In particular, they argued that if V_{max} increased with exposure (in a tissue region- and dose-specific manner), then it was possible to explain the naïve

[9] Note that Conolly et al. (2000) stated that they used the pre-exposed data, but this statement appears to be in error (see Subramaniam et al. [2007]).

vs. pre-exposed data of Casanova et al. (1994), with the value of k_{loss} effectively measured in vitro by Quievryn and Zhitkovich (2000). Furthermore, this value was measured directly, rather than obtained by indirect interpretation of measurements made at only two time points where significant changes in the tissue had occurred. Therefore, Subramaniam et al. (2007) considered the use of this lower value for k_{loss} to be more appropriate. Consequently, they re-implemented and re-optimized the Conolly et al. (2000) model with this modification and found that the fit so obtained to the acute DPX data was excellent. The re-implemented model will be used in this assessment, and more details can be found in Subramaniam et al. (2007).

It should be noted that this slower DPX repair rate was obtained in an in vitro study by using human cell lines that were transformed and immortalized. However, it appears that DPX repair in normal cells would be even slower. When non-transformed freshly purified human peripheral lymphocytes were used instead, the half-life for DPX repair was about 50% longer than in the cultured cells (Quievryn and Zhitkovich, 2000).

3.6.6.3.2. *Statistical uncertainty in parameter estimates and extrapolation.* Klein et al. (2009) developed methods for deriving statistical inferences of results from PBPK models. They used the Conolly et al. (2000) model for this purpose, specifically because of the sparse time-course information in the above DPX data. However, they used the value of k_{loss} deduced from Quievryn and Zhitkovich (2000) and fitted the model simultaneously to both the rat and rhesus monkey data, as opposed to the sequential fitting in Conolly et al. (2000). They found that the predicted DPX concentrations were extremely sensitive to V_{max} and tissue thickness as was also concluded by Georgieva et al. (2003) and Cohen-Hubal et al. (1997). K_m was seen to be substantially different across species, a finding that was attributed plausibly to the involvement of more than one enzyme (Klein et al., 2009; Georgieva et al., 2003). Klein et al. (2009) concluded that the two efforts (Conolly et al. [2000] vs. Klein et al. [2009]) resulted in substantially different predictions outside the range of the observed data over which the models were calibrated.

The differences between these models occur in spite of the fact that both methods use all the available DPX data in both species and the same model structures. At the 0.1 ppm exposure concentration, in general these authors obtained three- to fourfold higher DPX concentrations averaged over a 24-hour period after exposure. Furthermore, the standard deviations in Klein et al. (2009) for V_{max} and K_m were an order of magnitude higher and that for k_f was 35-fold lower than the corresponding standard deviations reported in Conolly et al. (2000). The relatively larger standard deviation for k_f resulted in this parameter becoming negative in Conolly et al. (2000) at even half the standard deviation below the maximum likelihood estimate (MLE) value.

Note that, at a negative value of k_f, formaldehyde would be produced as opposed to being cleared through its intrinsic reactivity.

Klein et al. (2009) concluded that these “remarkable differences outside the range of the observed data suggest caution in the use of these models in a predictive sense for extrapolating to human exposures.”

3.6.7. Uncertainty in Prediction of Human DPX Concentrations

Conolly et al. (2000) used both the rat and rhesus monkey data to predict human DPX concentrations and constructed a PBPK model for the rhesus monkey along similar lines as for the F344 rat. In the rhesus monkey model, they maintained the same values of k_b, k_{loss}, and k_f as in the rat model but optimized the values of V_{max} and K_m against the rhesus monkey data from Casanova et al. (1994). The rat and rhesus monkey parameters were then used to construct a human model (see Conolly et al. [2000] for a more detailed report of implementing the rhesus monkey model and the extrapolations to the situation in humans).

For the human, the model used the value of K_m obtained in the rhesus monkey model and the epithelial thickness averaged over three regions of the rhesus monkey nose. The maximum rate of metabolism, V_{max}, which was estimated independently for the rat and rhesus monkey by fitting to the DPX data available for these species, was then extrapolated to the human by assuming a power law scaling with body weight (BW) (i.e., $V_{max} = a \times BW^b$), and the coefficient “a” and exponent “b” were derived from the independently estimated values of $(V_{max})_{RAT}$ and $(V_{max})_{MONKEY}$. Table 3-7 gives the values of V_{max} and K_m in the Conolly et al. (2000) extrapolation.

Table 3-7. Extrapolation of parameters for enzymatic metabolism to the human

Parameter	F344 rat	Rhesus monkey	Human
V_{max} (pmol/min-mm^3)	1,008.0	91.0	15.7
K_m (pmol/mm^3)	70.8	6.69	6.69

Source: Conolly et al. (2000).

The extent of mechanistic data across species, as available in this case, is rarely seen with other chemicals, and the above scale-up procedure was an attempt to use both the rodent and primate DPX data. However, allometric relationships across species are generally based on regressing data from multiple species and usually multiple sources of data points. Thus, the empirical strength of a power law derived by using two data points (F344 rat and rhesus monkey) is extremely weak for use as an allometric relationship that can then be used to extrapolate to the human.

The following observations indicate the high level of uncertainty in the values of the parameters V_{max} and K_m in the Conolly et al. (2000) models for predicting DPXs. First, K_m varies by an order of magnitude across the rat and monkey models but is then considered invariant between the monkey and human models (Conolly et al., 2000). Second, the values in Conolly et al. (2000) for V_{max}/K_m, the low-dose limit of the rate of enzymatic metabolism, is roughly similar between the rat and monkey but lower by a factor of six in the human.

Another factor that can substantially influence the above extrapolation of DPXs in the human is that Conolly et al. (2000) assumed the tissue to be a well-mixed compartment with regard to formaldehyde interaction with DNA and used the amount of formaldehyde bound to DNA per unit volume of tissue as the DPX dose metric. Considering formaldehyde's highly reactive nature, the concentrations of formaldehyde and DPX are likely to have a sharp gradient with distance into the nasal mucosa (Georgieva et al., 2003). Given the interspecies differences in tissue thickness, there is consequent uncertainty as to whether DPX per unit volume or DPX per unit area of nasal lining is the more appropriate dose metric to be used in the extrapolation. In particular, it may be assumed that the cells at risk for tumor formation are only those in the epithelium and that measured DPX data (in monkeys and rats) are an average over the entire tissue thickness. Since the epithelial DPXs in monkeys (and presumably humans) would then be more greatly "diluted" by lower levels of DPX formation that occur deeper into the tissue than in rats, it could be predicted that the ratio of epithelial to measured DPXs in monkeys and humans would be much higher than the ratio in rats.

End of Volume I